Biochemistry

Perspective

Cite This: *Biochemistry* 2019, 58, 5198−5220

pubs.acs.org/biochemistry

Methyl (Alkyl)-Coenzyme M Reductases: Nickel F-430-Containing Enzymes Involved in Anaerobic Methane Formation and in Anaerobic Oxidation of Methane or of Short Chain Alkanes

Rudolf K. Thauer*

Max Planck Institute for Terrestrial Microbiology, Karl-von-Frisch-Strasse 10, Marburg 35043, Germany

ABSTRACT: Methyl-coenzyme M reductase (MCR) catalyzes the methane-forming step in methanogenic archaea. The active enzyme harbors the nickel(I) hydrocorphin coenzyme F-430 as a prosthetic group and catalyzes the reversible reduction of methyl-coenzyme M (CH_3−S-CoM) with coenzyme B (HS-CoM) to methane and CoM-S−S-CoB. MCR is also involved in anaerobic methane oxidation in reverse of methanogenesis and most probably in the anaerobic oxidation of ethane, propane, and butane. The challenging question is how the unreactive CH_3−S thioether bond in methyl-coenzyme M and the even more unreactive C−H bond in methane and the other hydrocarbons are anaerobically cleaved. A key to the answer is the negative redox potential (E_o') of the Ni(II)F-430/Ni(I)F-430 couple below −600 mV and the radical nature of Ni(I)F-430. However, the negative one-electron redox potential is also the Achilles heel of MCR; it makes the nickel enzyme one of the most O_2-sensitive enzymes known to date. Even under physiological conditions, the Ni(I) in MCR is oxidized to the Ni(II) or Ni(III) states, e.g., when in the cells the redox potential (E') of the CoM-S−S-CoB/HS-CoM and HS-CoB couple (E_o' = −140 mV) gets too high. Methanogens therefore harbor an enzyme system for the reactivation of inactivated MCR in an ATP-dependent reduction reaction. Purification of active MCR in the Ni(I) oxidation state is very challenging and has been achieved in only a few laboratories. This perspective reviews the function, structure, and properties of MCR, what is known and not known about the catalytic mechanism, how the inactive enzyme is reactivated, and what remains to be discovered.

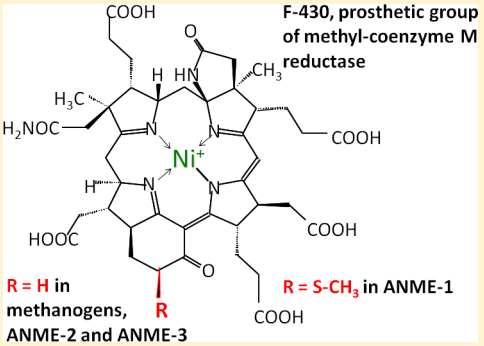

Methyl-coenzyme M reductase (MCR), which is composed of the subunits McrA (~65 kDa), McrB (~45 kDa), and McrG (~35 kDa), was discovered in the laboratory of Ralph Wolfe at the University of Illinois in the 1970s when studying methane formation in cell extracts of *Methanobacterium thermoautotrophicum* strain Δ*H* (renamed *Methanothermobacter thermoautotrophicus*), an archaeon that grows with H_2 and CO_2 as sole carbon and energy sources, forming methane. The Urbana group found that methyl-coenzyme M (CH_3−S-CoM) is reduced in cell extracts by H_2 in an ATP-dependent reaction[1−3] involving the three components A, B, and C,[4,5] of which component C turned out to be the methyl-coenzyme M reductase (MCR) per se[6−8] and component B to be 7-mercaptoheptanoylthreonine phosphate[9,10] that was later named coenzyme B (HS-CoB). Subsequently, it was shown that besides methane also the heterodisulfide CoM-S−S-CoB is formed (Figure 1).[11,12] Final evidence that CoM-S-S-CoM is a product was provided by Hedderich et al.,[13] 1989 in Marburg: the enzyme heterodisulfide reductase (HdrABC) was discovered that specifically catalyzes the reduction of CoM-S−S-CoB to HS-CoM and HS-CoB. Most of the enzymes involved in the biosynthesis of coenzyme M and coenzyme B are unique to methanogenic archaea.[14]

In 1979, the growth of methanogens was found by Schönheit et al.[17] in Marburg to be dependent on nickel. This finding led in 1980 to the discovery of nickel in F-430.[18,19] The nickel-containing, nonfluorescent compound, yellow in its Ni(II) and greenish in its Ni(I) oxidation states, was shown to be the prosthetic group of MCR[20] and to be a nickel tetrapyrrole.[21−24] The structure of the nickel hydrocorphin coenzyme F-430 (Abstract graphic; R = H) was elucidated in collaboration with the group of Albert Eschenmoser at the ETH Zürich.[25−28] (For the history, see ref 29.) Alternative structural proposals[30] were not confirmed.[31] The nickel in the prosthetic group has to be in the 1+ oxidation state for the enzyme to be active.[32,33] The genes and enzymes involved in the biosynthesis of coenzyme F-430 have been elucidated only recently.[34,35]

The first 20 years of MCR research were hampered by the fact that the specific activity of this enzyme in cell extracts was less than 0.1% of that expected from *in vivo* specific rates of methane formation. This led to many misleading results. It took to the early 1990s until it was found in Marburg how to obtain and purify active MCR with its F-430 to almost 100% in

Special Issue: Current Topics in Mechanistic Enzymology 2019

Received: February 27, 2019
Revised: March 21, 2019
Published: April 5, 2019

DOI: 10.1021/acs.biochem.9b00164
Biochemistry 2019, 58, 5198−5220

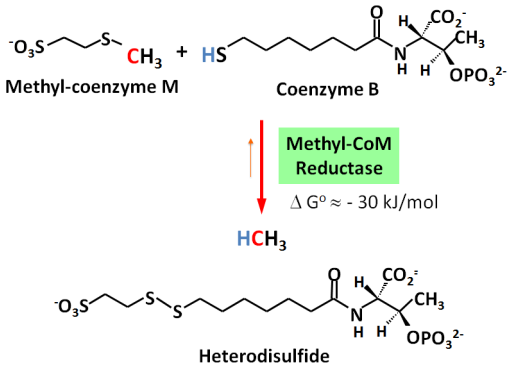

Figure 1. Reaction catalyzed by methyl-coenzyme M reductase that in the active form has a greenish color derived from Ni(I)F-430. Ni(I)F430 has a λ_{max} = 382 nm and a weaker maximum at 754 nm.[15] In the inactive state, MCR is yellow from Ni(II)F-430 that has an absorbance maximum at 430 nm. When MCR catalyzes the reduction of methyl-coenzyme M with coenzyme B in 100% D_2O, DCH_3 and some D_2CH_2 are formed. When MCR catalyzes CH_4 oxidation to methyl-coenzyme M in 100% D_2O, only CH_3–S-CoM is formed. It follows that the intermediates in the catalytic cycle do not exchange hydrogen with deuterium of the solvent. The hydrogen or deuterium atoms involved in the reaction are carried into the active site only via the thiol group of coenzyme B or, in the reverse reaction, via methane.[16] The standard free energy change (ΔG°) associated with ethane formation from ethyl-coenzyme M and coenzyme B is near −20 kJ/mol and thus by −10 kJ/mol less exergonic than ΔG° = −30 kJ/mol associated with methane formation from methyl-coenzyme M and coenzyme B (see the paragraph on "Reversibility").

the active, Ni(I) oxidation state.[32,33] Only from then on, real biochemical investigations were possible.

In 2010, we could finally demonstrate that purified MCR from *Methanothermobacter marburgensis* (formerly *Methanobacterium thermoautotrophicum* strain Marburg) also catalyzes the back reaction, the oxidation of methane to methyl-coenzyme M, at rates sufficient to account for observed rates of anaerobic methane oxidation *in vivo* (Figure 1).[36] This was important to show since the beginning of the 2000s evidence had accumulated that MCR is present in anaerobic methanotrophic archaea and that MCR therefore could be involved in the anaerobic oxidation of methane (AOM).[37,38] The anaerobic monofunctionalization of methane sparked the interest of biochemists and chemists in the catalytic mechanism of MCR because the homolytic cleavage of the first hydrogen of methane (439 kJ/mol) is very endergonic and by 18 kJ/mol more endergonic than of the second one.[39]

The "Biochemistry of Methyl-Coenzyme M Reductase" has recently been reviewed by Stephen Ragsdale at the University of Michigan, Ann Arbor, in the book "The Biological Chemistry of Nickel".[40] The book chapter focuses on experimental results obtained in the Ragsdale laboratory with respect to the catalytic mechanism of MCR. The present perspective has a broader scope. It aims at providing the reader with the understanding of why and where our present knowledge of MCR is incomplete.

The perspective begins with each a section on the role of MCR in the global carbon cycle, on the phylogeny of MCR and on *M. marburgensis* as a model organism for the MCR study. Sections on activity and the oxidation state of nickel in MCR follow as well as sections on localization, isoenzymes, and structural features. The discussion of the catalytic properties and the proposed catalytic mechanisms is followed by that of the individual steps of the catalytic cycle. A section dealing with proton inventories highlights how important it would be to know the solvent isotope effect (H_2O/D_2O) more precisely. A section on half-of-the sites reactivity brings together structural and catalytic features. Finally, it is summarized what is known about the reactivation mechanism.

■ ROLE OF MCR IN THE GLOBAL CARBON CYCLE

Methane is an important intermediate in the global carbon cycle (Figure 2).[41,42] About 1 Gt methane per year is formed in

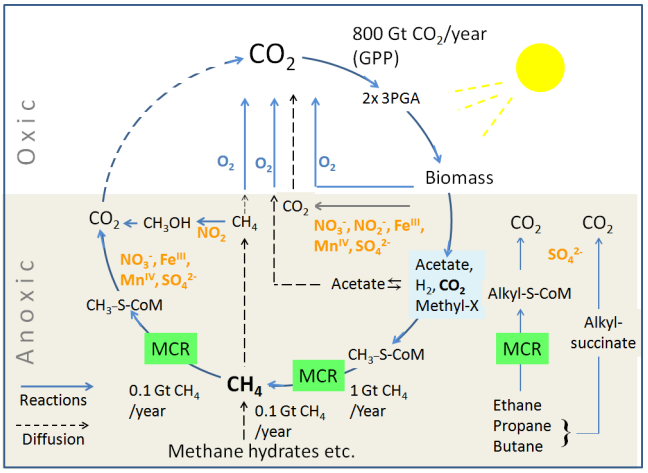

Figure 2. Role of methyl-coenzyme M reductase (MCR) in the global carbon cycle. GPP, gross primary production. Terrestrial GPP ≈ 500 Gt CO_2/year.[51] Marine GPP ≈ 300 Gt C/year.[52] Methyl-X, methanol, methylthiol, methylamines, choline, and betaine. 3-PGA, 3-phosphoglycerate. Electron acceptors for anaerobic methane oxidation are highlighted in orange. For a review on the anaerobic oxidation of ethane, propane, and butane, see Singh et al., 2017.[53]

anoxic environments from CO_2 and H_2, acetate, methylamines, and methanol by methanogenic archaea involving MCR.[42] An estimated amount of 0.1 Gt methane diffuses per year from deeply buried methane deposits into the anoxic biosphere. From the 1.1 Gt methane per year, about 0.1 Gt per year is oxidized with sulfate, Fe(III), Mn(IV), and nitrate to CO_2[43−45] involving MCR[46,47] (Figure 2). About 1 Gt methane per year diffuses into oxic environments, where about 60% is oxidized with O_2 to CO_2 by aerobic bacteria involving two types of methane monooxygenases (MMO), the iron enzyme sMMO ("s" for soluble), and the copper enzyme pMMO ("p" for particulate).[48] The other 40% escapes into the atmosphere, where methane is photo-oxidized to CO_2 involving OH radicals.[49] The concentration of methane in the atmosphere has more than doubled within the last 200 years (from 700 to 1875 ppb), which is of concern since methane is a potent greenhouse gas.[50]

MCR is not only involved in anaerobic methane formation and anaerobic oxidation of methane (AOM) but also appears to be also involved in the anaerobic oxidation to CO_2 of short chain alkanes such as butane, propane,[54] and ethane[55] by archaea (Figure 2). In the metagenome of ca. *Syntrophoarchaeum butanivorans* and ca. *S. caldarius*, which were both enriched on butane plus sulfate, and in the metagenomes of ca. *Agroarchaeum ethanivorans*, which was enriched on ethane plus sulfate, all of the genes required to synthesize active MCR were not only found but also found to be expressed. Most importantly, the cells were shown to contain the respective

DOI: 10.1021/acs.biochem.9b00164
Biochemistry 2019, 58, 5198−5220

alky-S-CoM intermediate, indicating that MCR in these archaea indeed catalyzes the oxidation of these alkanes. Upon incubation with methane, the cells did not form methyl-coenzyme M, suggesting that the MCR might be able to discriminate against methane.[54,55]

Due to the low specific activity of MCR in catalyzing methane oxidation, the enzyme has to be present in methanotrophic archaea in very high concentrations (>10% of the cytoplasmic protein).[38] After RuBisCo,[56] MCR is estimated to be one of the most abundant enzymes on Earth. In anoxic sediments catalyzing AOM, the presence of F-430 can easily be detected and quantified.[57−59] MCR could even be purified and crystallized from microbial mats catalyzing AOM.[38,60]

MCR PHYLOGENY

Until 2003, MCR was considered to be present only in the five orders of methanogens then known: Methanobacteriales, Methanococcales, Methanomicrobiales, Methanopyrales, and Methanosarcinales.[61] From the year 2003 and on, using the *mcrA* gene as a genetic marker (Figure 3.),[62,63] the list of archaea containing MCR extended to archaea catalyzing the anaerobic oxidation of methane (ANME).[37] In 2007, the candidate order ANME was split up in the candidate's orders of ANME-1, ANME-2, and ANME-3.[64] In 2008, the MCR-containing order of Methanocellales (uncultured archaeal group rice cluster I) was inaugurated.[65] In 2014, the *mcr* genes were found in methanogenic archaea of the new order Methanomassiliicoccales that are closely related to the Thermoplasmatales[66,67] in 2016 in archaea that can oxidize butane and that are distantly related to ANME-1,[54] in 2017 in methanogenic archaea closely related to Haloarchaea,[68] and in 2019 in archaea that can oxidize ethane with sulfate and that are distantly related to the Methanosarcinales.[55] (See also ref 69.)

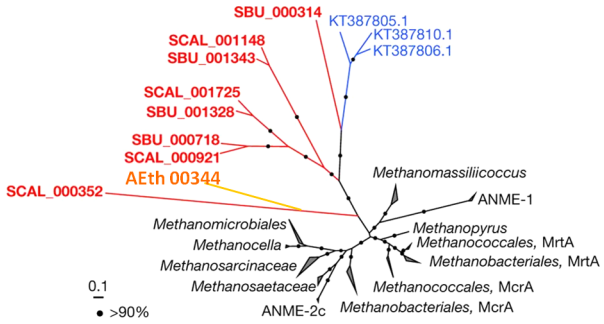

Figure 3. Phylogenetic relation of McrA amino acid sequences present in Euryarchaeota (black, red, and orange branches) and in Bathyarchaeota (blue branches). The phylogenetic tree was constructed based on a maximum likelihood algorithm considering more than 450 amino acid positions. The scale bar indicates the number of amino acid substitutions per site. Bootstrap values higher than 90% are indicated by filled circles on the corresponding branch. Black branches, sequences from methanogens and methanotrophic archaea. Red branches, sequences from ca. Syntrophoarchaeum;[54] SBU, ca. *S. butanivorans*; SCAL, ca. *S. caldarius*. Orange branch, sequence from ca. *Argoarchaeum ethanivorans*.[55] Blue branches indicate *Bathyarchaeota*-related sequences.[70] The identifiers refer to the locus tag of the gene sequences in the draft genomes. MrtA is synonymous to McrA isoenzymes II in the corresponding groups. The figure and legend are taken from Laso-Peres et al., 2016,[54] (with permission of Nature-Springer), and updated by the orange branch with the branching order taken from Chen et al., 2019.[55]

All of these MCR-containing orders mentioned above belong to the kingdom of Euryarchaeota (Figure 3, black, red, and orange branches). But recent findings indicate that MCR is not restricted to this kingdom because metagenomes of archaea belonging to the Bathyarchaeota were found to contain the genes for a functional MCR (Figure 3, blue branches).[70−72] However, outside the domain of archaea, *mcr* genes have not yet been found.

M. MARBURGENSIS: THE MODEL ORGANISM USED FOR THE STUDY OF MCR

Most of what is known about the biochemistry of MCR comes from studies of isoenzyme I from *M. marburgensis* that thrives on a completely mineral salts medium with 80% H_2 and 20% CO_2 as a sole energy source. Its energy metabolism is outlined in Figure 4. *M. marburgensis* was isolated in 1978 by Georg Fuchs from the municipal anaerobic digestion plant in Marburg.[73] It grows optimally at 65 °C with a doubling time of below 2 h to a cell concentration of 2.5 g dry mass per liter[74] and contains MCR up to 10% of the cellular proteins From such grown cells, the nickel enzyme is relatively easy to purify.[33]

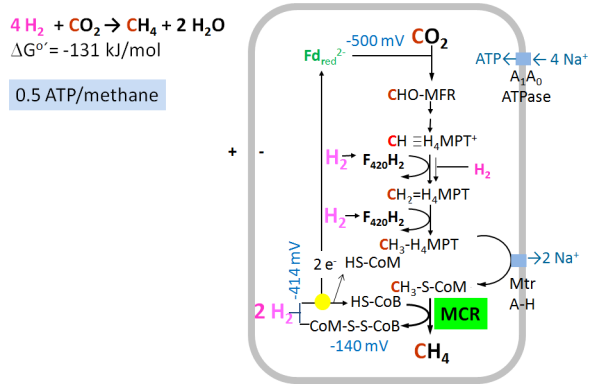

Figure 4. Energy metabolism of *Methanothermobacter marburgensis*. MFR, methanofuran. H_4MPT, tetrahydromethanopterin. F_{420}, coenzyme F_{420}. HS-CoM, coenzyme M. HS-CoB, coenzyme B. Fd, ferredoxin. MCR, methyl-coenzyme M reductase. Yellow dot, heterodisulfide reductase- hydrogenase complex (HdrABC-MvhADG) that couples the exergonic reduction of CoM-S−S-CoB with H_2 with the endergonic reduction of ferredoxin with H_2 via flavin-based electron bifurcation.[42,75−78] The redox potentials, in blue, are given under standard conditions.

INACTIVATION OF MCR WHEN IN THE CELLS THE REDOX POTENTIAL OF THE COM−S−S-COB/HS-COM PLUS HS-COB COUPLE BECOMES TOO HIGH

To obtain active MCR, cultures of *M. marburgensis* grown on 80% H_2 and 20% CO_2 must be exposed to 100% H_2 before harvest. Only then the cells contain mainly active MCR that exhibits the electron paramagnetic resonance (EPR) signal designated as MCR-red1.[32,79] To the contrary, when the cells are exposed to 80% N_2/20% CO_2 prior to harvest, MCR is inactive and exhibits the EPR signal MCR-ox1.[33,79] When the cells are directly harvested, the MCR is inactive and EPR-silent. An explanation for the observed effects can probably be

DOI: 10.1021/acs.biochem.9b00164
Biochemistry 2019, 58, 5198−5220

found in the differences in intracellular concentrations of CH_3−S-CoM, HS-CoM, HS-CoB, and CoM-S−S-CoB. The redox potential E_o' of the CoM-S−S-CoB/HS-CoM + HS-CoB couple under standard conditions is −140 mV.[80]

When only H_2 rather than CO_2 is present, then high intracellular concentrations of HS-CoM and HS-CoB and essentially zero concentration of CoM-S−S-CoB are to be expected; in the absence of CO_2, methyl-coenzyme M cannot be regenerated (Figure 4); the redox potential of the CoM-S−S-CoB/HS-CoM + HS-CoB couple under these conditions will be much more negative than −140 mV. Vice versa, when the cells are gassed with CO_2 in the absence of H_2 before harvest, the concentrations of HS-CoM and HS-CoB will be essentially zero and that of CoM-S−S-CoB very high; in the absence of H_2, the heterodisulfide CoM-S−S-CoB cannot be reduced (Figure 4); the redox potential of the CoM-S−S-CoB/HS-CoM + HS-CoB couple under these conditions will be substantially more positive than −140 mV. Finally, when the cells are directly harvested, there is an intermediary situation with a redox potential of the CoM-S−S-CoB/HS-CoM + HS-CoB couple probably near −140 mV. It thus appears that MCR in *M. marburgensis* cells is only in its active state when the redox potential of the CoM-S−S-CoB/HS-CoM + HS-CoB couple is considerably more negative than the standard redox potential of −140 mV.

OXIDATION STATES OF NICKEL IN MCR

F-430 in MCR can be in the Ni(I), Ni(II), and Ni(III) oxidation state, of which the Ni(I) state (MCR-red) and Ni(III) state (MCR-ox) show characteristic EPR spectra, as first revealed in 1988 by Simon Albracht at the University of Amsterdam.[79] The Ni(II) state is EPR-silent (MCR-silent). The three states can also be distinguished by UV−visible spectroscopy.[81−83]

Active MCR in the Red1 State. *M. marburgensis* cells growing exponentially at 65 °C on 80% H_2/20% CO_2 with a doubling time of 2 h form methane at a specific rate of 10 μmol min^{-1} mg $protein^{-1}$. Extracts of such grown cells are therefore expected to catalyze methane formation from methyl-coenzyme M and coenzyme B at a specific activity of at least 10 μmol min^{-1} mg $protein^{-1}$. For many years, however, only specific activities below 0.1 μmol min^{-1} mg $protein^{-1}$ were observed. The breakthrough came from the finding that cell suspensions of *M. marburgensis* exhibited a strong MCR-red1 signal when incubated under 100% H_2[79] and that extracts of such H_2-reduced cells catalyzed methyl-coenzyme M reduction with coenzyme B at specific rates near 2 μmol min^{-1} mg $protein^{-1}$.[32] After 10-fold purification in the presence of the competitive inhibitor coenzyme M to stabilize the activity, the purified enzyme-catalyzed methane formation from methyl-coenzyme M and coenzyme B at a specific activity of about 20 μmol mn^{-1} mg $protein^{-1}$. The purified MCR I had a greenish color with a maximum at 386 nm and exhibited the axial MRC-red1 signal (g_1 = 2.25; g_2 = 2.07; g_3 = 2.06) with a spin concentration near 0.2. The EPR and UV−visible spectra of MCR-red1 compared amazingly well with those exhibited by the penta-methyl ester of Ni(I)F-430 (Ni(I)F-430M).[84] It was therefore concluded that in MCR-red1 the nickel is in the 1+ oxidation state. Upon inactivation of active MCR with chloroform, the spin concentration and the specific activity decreased in parallel, from which it was concluded that nickel in MCR has to be in the 1+ oxidation state to be active.[32]

The one-electron, reversible reduction potential (E_m') of Ni(II)F-430M/Ni(I)F-430 couple in dimethylformamide was found to be −504 mV versus the hydrogen electrode (0.0 V)[15,84] and that of F-430 in water to be −650 mV.[85] Oxidation of MCR-red1 with ferricyanide yielded a one-electron Nernst plot with $E_{m_{7.2}}$ = −440 mV, but the oxidation was irreversible.[82] The redox potential of the MCR-bound F-430 is probably considerably lower than those of the free F-430 M in acetonitrile due to the difference in coordination, four coordinates in free F-430M, five coordinates in MCR-red1a, and six coordinates in MCR-silent (see below).

Inactive MCR in the Ox1 State. After growth of *M. marburgensis* on 80% H_2/20% CO_2, the cultures were gassed with 80% N_2/20% CO_2 before cooling and harvesting; the cell extracts exhibited a strong MCR-ox1 EPR signal (g_1 = 2.2310; g_2 = 2.1667; g_3 = 2.1532)[82] and showed essentially no MCR activity.[33,79] Instead of gassing the cultures with 80% N_2/20% CO_2, it is also possible to induce the MCR-ox1 signal by adding 20 mmol sodium sulfide per liter culture before the harvest; this was shown for *M. marburgensis* and *Methanosarcina thermophila*.[86] The ox1 EPR signal of inactive MCR was, as the red1 EPR signal of active MCR, quenched by O_2, chloroform, or nitric oxide, but only at much higher concentrations and lower rates.[87] MCR in the ox1 state is therefore relatively easy to purify to apparent homogeneity with almost 100% of its Ni in the ox1 state. Upon reduction of MCR-ox1 in the presence of methyl-coenzyme M with titanium(III) citrate at pH 9, inactive MCR-ox1 was almost 100% converted to active MCR-red1. Specific activities of up to 100 μmol min^{-1} mg $protein^{-1}$ were reached.[33] The requirement of the strong reductant Ti(III) for the conversion of MCR-ox1 to MCR-red1 was interpreted to indicate that in MCR-ox1 the nickel is in the 3+ oxidation state.[33]

This interpretation was subsequently challenged by the group of Steven Ragsdale, which proposed that, as in the red1 state, the nickel in MCR-ox1 is in the 1+ oxidation state.[88] One valid argument was that the EPR spectrum of the pentamethylester of Ni(III)F-430 in aprotic solvent[89] was completely different from that of MCR in the ox1 state.[33] The one-electron reversible oxidation potential of F-430 M in dimethylformamide was measured to be +625 mV.[89] In view of the high oxidation potential, four-coordinate or axially weakly coordinated forms of Ni(III)F-430 were considered unlikely to be of biological importance.[15] A counter argument was that the axial coordination of a strong donor like a thiolate or a CH_3^- anion to Ni(III)F-430 in MCR could change the spectra and lower the oxidation potential sufficiently.[89] Indeed, the spectra of MCR in the ox state, in which the Ni(III) in F-430 is either thiolated (CoM-S-Ni(III)F-430)[90] or methylated (methyl-Ni(III)F-430)[91,92] are, as expected, quite different from Ni(III)F-430 M in acetonitrile.[89] Another valid argument was that MCR-silent could be converted to the ox1 state by irradiation under cryo-conditions.[93]

To explain the Ti(III) reduction results, it was postulated that upon reduction of MCR in the ox1 state to the red1 state, the hydrocorphin ring of F-430 rather than the nickel was reduced by two electrons and experimental evidence for this was provided.[87,94] However, later these experimental findings were reevaluated.[95−98] There is now general agreement that in the ox1 state the thiol sulfur of coenzyme M forms a bond to N(III), in which the Ni(III) thiolate and Ni(II) thiyl radical are in equilibrium.[81,97]

DOI: 10.1021/acs.biochem.9b00164
Biochemistry 2019, 58, 5198−5220

Inactive MCR in the Ox2 and Ox3 States. Addition of Na_2SO_3 to MCR in the red2 state (see below) was found to induce the light-sensitive EPR signal designated as MCR-ox2 (g_1 = 2.2263; g_2 = 2.1425; g_3 = 2.1285),[82] and exposure of MCR in the red2 state to O_2 was found to induce the light-sensitive EPR signal MCR-ox3a (g_1 = 2.2170; g_2 = 2.1400; g_3 = 2.1340).[82] Induction of the two ox signals is irreversible in the sense that removal of Na_2SO_3 or O_2 did not restore the red2 state. The light sensitivity discriminates MCR-ox2 and MCR-ox3 from MCR-ox1, which is not light-sensitive.[82] The nickel in MCR-ox2 and MCR-ox3 is, as in MCR-ox1, most likely also in the 3+ oxidation state although this has not been analyzed in detail.

CYTOPLASMIC LOCATION AND ISOENYZMES

Cytoplasmic Location. Although MCR is found primarily in the soluble cell fraction, whole-cell immune-labeling experiments with *Methanosarcina*[99] and *Methanothermobacter*[100,101] have indicated that the enzyme is membrane associated. (See also ref 102.) Localization close to the cytoplasmic membrane was confirmed recently.[103] However, none of the genes associated with MCR synthesis are predicted to code for proteins that have a membrane anchor. Localization close to the membrane is therefore probably by another mechanism that remains to be elucidated.

Isoenzymes. *M. marburgensis* contains two MCR isoenzymes that are differently expressed in different growth phases: MCR I is synthesized when, during growth on H_2 and CO_2, the H_2 supply is limiting at high cell concentrations and MCR II when H_2 is repleted.[104−106] The two isoenzymes can be separated by chromatography on anion exchange resins; the one that eluted first was designated as MCR II and the one that eluted second MCR I. At the gene level, the two isoenzymes are referred to as *mrt* (MCR II) and *mcr* (MCR I).[106] The two isoenzymes, which both exhibit a ternary complex kinetic mechanism, were found to mainly differ in their K_M for methyl-coenzyme M and coenzyme B and their pH optimum (see below).[107] Almost all of the experiments to resolve the catalytic mechanism were performed with MCR I because this isoenzyme is present in the highest concentrations in the archaeon at the end of exponential growth when the H_2 supply becomes limiting and the cells are harvested.

M. marburgensis is not the only methanogen that contains two MCR isoenzymes. Also many other members of the Methanobacteriales, many members of the Methanococcales, and a few members of the Methanomicrobiales contain two MCR isoenzymes. Phylogenetic analyses on the basis of all three subunits grouped MCRs from Methanobacteriales and Methanococcales into three distinct types: (i) MCRs found only in Methanobacteriales; (ii) MCRs found in Methanobacteriales and Methanococcales; and MCR found only in Methanococcales. The first and second types include the MCR isoenzymes I and II, respectively, from *M. marburgensis*.[61] The three types are structurally highly similar with respect to the overall fold and active site architecture including the structure and binding mode of F-430 and the substrates. However, the MCRs significantly differ regarding the electrostatic surface potentials (which is why they can be separated by anion exchange chromatography), the loop architectures, and in particular the C-terminal end of their McrG subunit that interact with the McrA and McrB subunits in a different manner, which could affect the kinetic properties.[61]

Members of the Methanosarcinales, Methanomassiliicoccales, Methanocellales, and the ANME 1−3 groups appear to contain only one type of MCR, but in the archaea that catalyzes the oxidation of butane four sets of *mcr* genes were found.[54]

STRUCTURAL FEATURES

Subunit Composition. MCR I is composed of three different subunits α (McrA), β (McrB), and γ (McrG), each being present twice. Per mol mass of up to 300 kDa, the enzyme contains 2 mol of the nickel hydrocorphin F-430 tightly but not covalently bound. The genes for the three subunits were found in the transcription units *mcrBGCDA* (isoenzyme I) and *mrtBGDA* (isoenzyme II).[108−110] McrC and McrD are not required for MCR activity[111] but apparently are required for post-translational assembly (McrD)[112] and activation of the enzyme (McrC).[113]

MCR from acetate-grown *Methanosarcina thermophila* was found to be an $\alpha_1\beta_1\gamma_1$ trimer with a native molecular mass of between 132 000 and 141 000 Da and to contain 1 F-430 bound.[114] MCR from *M. thermophila* thus appears to differ from all other investigated MCRs, which are $\alpha_2\beta_2\gamma_2$ hexamers. Because of the intertwined hexameric structure (see below), a dissociation of the hexamer into two trimers is difficult to envisage. It would be therefore very interesting to obtain a crystal structure of this MCR.

Coenzyme B Bound to an UDP-Disaccharide? Evidence was published in beginning of the 1990s that showed coenzyme B (Figure 1) is covalently bound to an UDP-disaccharide through a carboxylic-phosphoric anhydride linkage and that this conjugated coenzyme B might actually be the real electron donor for methyl-coenzyme M reduction to methane.[115,116] Since the cell extracts used to test this proposed substrate had only specific activities of methane formation in the nmol min^{-1} mg $protein^{-1}$ range, the validity of the results is difficult to judge. In crystal structures of MCR with coenzyme B bound, such a carbohydrate moiety was carefully looked for but never observed (see below).

Crystal Structures of MCR from Methanogens. In collaboration with Ulrich Ermler at the Max Planck Institute for Biophysics in Frankfurt, Seigo Shima in Marburg obtained in 1997, two crystal structures of inactive MCR I from *M. marburgensis*. The crystal structure of MCR-ox1-silent with coenzyme M and coenzyme B bound (Figure 5A) was resolved

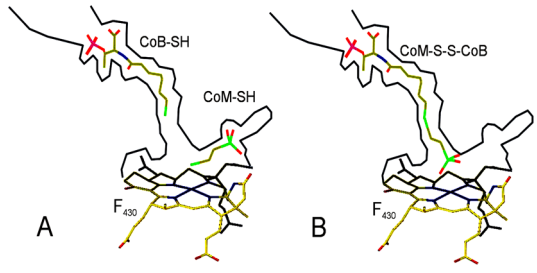

Figure 5. Schematic drawing of the active site of inactive methyl-coenzyme M reductase (MCR) with F-430 in the Ni(II) oxidation state based on crystal structures up to 1.1 Å resolution of isoenzymes I from *M. marburgensis*. (A) MCR-ox1-silent, MCR in complex with coenzyme M (CoM-SH) and coenzyme B (CoB-SH). (B), MCR-silent, MCR with the heterodisulfide CoM-S−S-CoB bound. Sulfur in green, carbon yellow, nickel in blue, and oxygen in red. From Mahlert et al., 2002.[83]

DOI: 10.1021/acs.biochem.9b00164
Biochemistry 2019, 58, 5198−5220

to 1.45 Å and the one of MCR-silent with CoM-S−S-CoB bound (Figure 5B) to 2 Å[117] and later refined to 1.16 and 1.8 Å, respectively.[118] A third structure, which MCR-red1-silent refined to 1.8 Å, was without any substrates or products bound.[118]

The three structures confirmed that the different subunits are arranged in an $\alpha_2,\beta_2,\gamma_2$ configuration and revealed two identical interconnected F-430-harboring active sites separated by 50 Å. The two F-430s are embedded deeply between the subunits $\alpha,\alpha',\beta,\gamma$ and $\alpha',\alpha,\beta',\gamma'$. Glutamine $\alpha'147$ provides the lower axial ligand to Ni(II) in F-430 that is mainly bound to the subunits α, β, and γ, and glutamine $\alpha147$ provides the lower axial ligand to Ni(II) in F-430 that is mainly bound to the subunits α', β', and γ'. Each active site is accessible from the surface only through a 50 Å long channel, which is 25 Å in diameter at the protein surface and narrows to 8 Å for the last 16 Å, which leads to a pocket at the base where F-430 binds. Through this channel, methyl-coenzyme M reaches F-430 and coordinates there axially with its thioether sulfur to the nickel from the front side. The channel is tightly locked after binding of the second substrate coenzyme B.[117,118] All attempts to obtain a crystal structure of active MCR failed until now because the Ni(I)F-430 in the active site always autoxidized to Ni(II) during the crystallization procedure even when performed in an anaerobic chamber containing O_2-free gas (95% N_2 + 5% H_2).

Crystal structures were later also published by the Ragsdale group. MCR-red1-silent structures with coenzyme B analogues (CoB_4SH to Cob_8SH) were obtained that allowed to map the 50 Å long channel.[119] A structure of MCR, in which the Ni(I) of F-430 is methylated by methyl iodide, forming a methyl-Ni(III)bond, showed no significant differences in the conformation of the active site as compared to the three MCR-silent structures, in which the Ni of F-430 is in the Ni(II) oxidation state.[120]

Comparison of the crystal structures of MCR from *M. marburgensis* with MCRs from the phylogenetically distant *Methanosarcina barkeri*, *Methanopyrus kandleri*,[121] *Methanotorris formicicus*, and *Methanothermococcus thermolithotrophicus*[61] revealed highly similar overall structures and virtually an identical active site architecture, reflecting the chemical challenging mechanism of methane formation. Pronounced differences were found, however, at the protein surface, loop geometries and electrostatic properties, which also involve the entrance of the active site funnel.[61]

Structure of MCR from Nonmethanogens. Also an X-ray structure of the 280 kDa heterohexameric MCR complex from an ANME-1 archaeon was obtained.[60] The enzyme complex was crystallized uniquely from a protein ensemble purified from consortia of microorganisms collected with a submersible from a Black Sea mat catalyzing AOM with sulfate.[38] Crystals grown from the heterogeneous sample diffracted to 2.1 Å resolution and consisted of a single ANME-1 MCR population, demonstrating the strong selective power of crystallization. The structure revealed ANME-1 MCR in complex with coenzyme M and coenzyme B, indicating identical substrates for MCR from methanotrophic and methanogenic archaea. Differences between the highly similar structures of ANME-1 MCR and methanogenic MCR include a F-430 structural modification with a methylthio group (R= S-CH_3 in the Abstract graphic),[122] a cysteine-rich patch in McrA and a somewhat altered post-translational amino acid modification pattern. However, the active site thioglycine and 1-*N*-methylhistidine were conserved (see below). The differences may tune the enzymes for their functions in different biological contexts.[60] In support of this possibility is the finding that recombinant *Methanosarcina acetivorans* containing *mcr* genes from an ANME-1 organism were more efficient in oxidizing methane with Fe(III) than the wild type.[123] Note, however, that MCR from ANME-2 and ANME-3 archaea contain normal coenzyme F-430.[122]

A screen for F-430 variants in cell extracts of various methanogens and ANME organisms revealed the presence of multiple modified F-430 structures. A total of nine modified F-430 structures were identified. It was not determined, whether these F-430 variants are associated with MCR or whether they may have another function is still to be determined.[124]

Unfortunately, only enrichment cultures of butane or ethane-oxidizing archaea are available to date. Therefore, all that is known of MCR from these archaea comes from metagenomes studies, by which the primary structure of the MCRs can be deduced. From homology modeling from the primary structures using the crystal structures of MCRs from methanogens, it was found that the MCR from butanotrophic and ethanotrophic archaea have overall three-dimensional structures very similar to those of MCRs from methanogenic archaea.[54,55] Differences were observed in the amino acid sequence of the catalytic pocket. However, these differences do not yet explain why MCR from ANME archaea appear to specifically catalyze the oxidation of methane, whereas the MCR from butane- or ethane-oxidizing archaea appear to specifically catalyze the oxidation of butane or ethane, respectively.[54,55]

Post-Translational Modifications. The subunit McrA of MCR I from *M. marburgensis* was shown to contain five post-translational modifications of active site amino acids: a thioglycine, 1-*N*-methyl-histidine, S-methyl-cysteine, 5-methyl-arginine, and 2-methy-glutamine.[117] The methyl group in the modified amino acids was shown to be derived from the methyl group of methionine most probably via S-adenosylmethionine.[125] Recently a sixth novel post-translationally modified amino acid, namely, didehydroaspartate, was found adjacent to the thioglycine as revealed by mass spectrometry and high-resolution X-ray crystallography. Upon chemical reduction, the didehydroaspartate residue was converted into aspartate.[61]

Most of the six modifications were found also in MCRs from other methanogens.[60,61,121,126] Especially the thioglycine and the 1-*N*-methylhistidine appear to be highly conserved, the latter probably because this modification is required for correct coenzyme B binding.[117] MCR III from *M. formicicus* lacks the S-methylcysteine but possesses in the α subunit a 6-hydroxytryptophane. Instead of a 2-methyl-glutamine there is a glutamine in McrA from *M. barkeri* and where there is a didehydroaspartate there is an aspartate in McrA from *Methanothermobacter wolfei*.[61]

In *Methanosarcina*, the genes responsible for the post-translational modification of the glycine to thioglycine[127−129] and for the conversion of the active site arginine to 5-methylarginine[130] were identified and individually deleted. The deletions were found to negatively affect growth of the methanogens, however, only under stress conditions. A role of the two highly conserved post-translational modifications in stabilizing the protein's secondary structure near the active site was proposed.[127,130] However, the specific activity and kinetic properties of the enzyme variants were not determined.

DOI: 10.1021/acs.biochem.9b00164
Biochemistry 2019, 58, 5198−5220

Whether the variant enzyme still shows full activity cannot be deduced from the *in vivo* growth experiments, as has been proposed, because it is not known whether *in vivo* the reduction of methyl-coenzyme M to methane via MCR was growth-rate limiting, which it most probably was not. Indeed, at the low-energy substrate concentrations prevailing in the natural habitats of methanogens, their energy metabolism is generally growth-rate limiting.[131] However, this is not the case at the much higher methanogenic substrate concentrations used in the laboratory to grow the archaea in batch cultures. This is evidenced by the fact that the growth rate and growth yield of *Methanosarcina* species in mineral salts media are increased when, for example, yeast extract and peptone are added, indicating that biosynthesis rather than the energy metabolism was growth-rate limiting. An interpretation of the mutation results thus has to await comparative measurements of the enzyme's catalytic efficiency (k_{cat}/K_M) and activation energy (temperature dependence of activity) and determination of whether the variant MCR still shows half-of-the-sites reactivity (see below).

Post-Translational Assembly. When the *mcrBGCDA* genes from the thermophile *Methanothermococcus okinawensis* were expressed in the mesophile *Methanococcus maripaludis*, the purified recombinant rMCR*ok* was found to be post-translationally modified correctly and to contain F-430 and McrD,[112] which in *Methanococcus* species is associated with the McrABG complex.[132] Subunits of the native *M. maripaludis* (MCR*mar*) were largely absent in the purified enzyme, even though MCR*mar* was produced in the cells, suggesting that the recombinant enzyme was formed by an assembly of cotranscribed subunits. Strong support for this hypothesis was obtained by expressing in *M. maripaludis* a chimeric operon, comprising the His-tagged *mcrA* from *M. maripaludis* and *mcrBDCG* from *M. okinawensis*. Indeed, the His-tagged MCR was found to contain *M. maripaludis* McrA and *M. okinawensis* McrBDG.[112]

CATALYTIC PROPERTIES AND INHIBITORS

The amino acid sequences of McrA, McrB, and McrG of isoenzymes I from *M. marburgensis*, which belongs to the *Methanobacteriales*, are significantly different from those of MCRs from other methanogens and methanotrophic archaea (Figure 3). Even the two isoenzymes of *M. marburgensis* share only about 70% sequence identity.[61] It is well-known that the substrate specificity and catalytic efficiency of phylogenetically closely related enzymes can differ. These properties are reliably known only for MCR I from *M. marburgensis*. It could therefore well be that MCR even from closely related methanogens differs significantly in catalytic properties.

Purified MCR I and MCR II from *M. marburgensis* in the active red1 state are difficult to obtain because in the presence of trace amounts O_2, which are difficult to exclude completely during purification, the red1 EPR signal is quenched. The Ni(I)F-430 in the active site is somewhat protected from oxidation in the presence of the MCR substrate methyl-coenzyme M or the substrate analogue coenzyme M.[133] However, even in the presence of methyl-coenzyme M or coenzyme M, loss of activity in the presence of O_2 is still rapid, which is why purifications have to be performed in anaerobic chambers containing O_2-free gas (95% N_2 + 5% H_2).

MCR I-red1, obtained from purified MCR-ox1 by reduction with Ti(III) in the presence of methyl-coenzyme M, catalyzed at 60 °C, the reduction of methyl-coenzyme M (apparent K_M = 0.7 ± 0.2 mM) with coenzyme B (apparent K_M = 0.2 ± 0.1 mM) to methane and CoM-S−S-CoB at a specific activity of up to 100 μmol min^{-1} mg protein^{-1} (apparent V_{max}).[33,107] MCR II-red1 differed in its kinetic properties from MCR I-red1: the apparent K_M for methyl-coenzyme M was 1.4 ± 0.2 mM and that for coenzyme B was 0.5 ± 0.2 mM. The pH optimum of MCR II was 7.5−8.0 as compared to 7.0−7.5 in the case of MCR I.[33,107]

When MCR I-red1 was purified in the presence of coenzyme M, the apparent K_M for methyl-coenzyme M was 5 mM rather than 0.7 mM and the apparent V_{max} was considerably lower than 100 μmol min^{-1} mg protein^{-1}, most probably because the preparations still contained coenzyme M that is an efficient reversible MCR inhibitor, inhibition being competitive to methyl-coenzyme M.[133]

Substrate Specificity. MCR I purified in the presence of coenzyme M also catalyzed the reduction of ethyl-coenzyme M (apparent K_M = 20 mM), albeit at a specific activity of only 0.1 μmol min^{-1} mg protein^{-1}. The enzyme did not catalyze the reduction of propyl-coenzyme M, of allyl-coenzyme M and of trifluoromethyl-coenzyme M.[133] Besides coenzyme B (7-mercaptoheptanoyl-threonine phosphate), also 6-mercaptohexanoyl-threonine phosphate ($HSCo_6B$) could serve as an electron donor; however, the rates of methyl-coenzyme M reduction with $HSCo_6B$ were less than 1% of the rates with $HSCo_6B$.[134,135] The slow substrate CoB_6−SH has been a valuable analogue in helping decipher the MCR catalytic mechanism.[136]

Stereospecificity. The reduction of ethyl-coenzyme M proceeds with inversion of stereoconfiguration as determined with an isotopically chiral form of ethyl-coenzyme M in cell extracts of *Methanosarcina barkeri*.[137] Studies with purified enzyme from *M. marburgensis*, in which the incorporation of deuterium from D_2O into the ethyl group of ethyl-coenzyme M was followed, are consistent with the inversion of stereoconfiguration.[138]

Cell extracts of *M. thermoautotrophicus* catalyzed, beside the reduction of methyl-coenzyme M and ethyl-coenzyme M with H_2, also the reduction of monofluoromethyl-coenzyme M, difluoromethyl-coenzyme M, methyl-selenocoenzyme M, and 3-methylthiopropionate. The relative rates observed are difficult to interpret because the specific activities even with methyl-coenzyme M were very low, and these low specific activities were only obtained in the presence of ATP, which was required to activate the two isoenzymes in the cell extracts.[139−141]

Reversibility. MCR I was shown to catalyze the back reaction, the oxidation of methane, with a specific activity of near 10 nmol min^{-1} mg protein^{-1} at 60 °C and 1 bar $^{13}CH_4$ (corresponding to about 1 mM methane at 60 °C), which is only about 0.01% of the specific activity of the forward reaction.[36] The rate of methane oxidation increased with the methane concentration linearly up to 2 mM, the highest concentration reached experimentally, indicating that the apparent K_M for methane is way above 2 mM. The kinetic properties of MCR from *M. marburgensis* are compatible with MCR being the enzyme that in the very slowly growing ANME organisms catalyzes the anaerobic oxidation of methane.[36]

The specific rate of methane oxidation (10 nmol min^{-1} mg protein^{-1}) (V_{-1}) is low relative to that of methane formation (100 μmol min^{-1} mg protein^{-1}) (V_{+1}): $V_{+1}/V_{-1} = 10^4$. The Haldane equation,[142] which relates the free energy change ($\Delta G°$) of −30 kJ/mol associated with the MCR-catalyzed

DOI: 10.1021/acs.biochem.9b00164
Biochemistry 2019, 58, 5198−5220

reaction (Figure 1) to the reaction's equilibrium constant, predicts that the catalytic efficiency (V_{max}/K_M) of the forward reaction (methane formation) divided by the catalytic efficiency of the back reaction (methane oxidation) should be somewhat above 10^5. Since the V_{max} and K_M for methane oxidation are not yet known, it cannot be decided whether $V_{+1}/V_{-1} = 10^4$ is a good match. Also, it has to be considered that $\Delta G^o = -30$ kJ/mol is only known with some uncertainty.

$\Delta G^o = 30$ kJ/mol was calculated from the ΔG^o of three reactions, namely, (i) methanol reduction with H_2 to methane ($\Delta G^o = -112.5$ kJ/mol),[131] (ii) CoM-S−S-CoB reduction with H_2 to HS-CoM and HS-CoB ($\Delta G^o = -53$ kJ/mol), and (iii) methyl-S-CoM formation from methanol and coenzyme M ($\Delta G^o = -26.5$ kJ/mol).[143] (Methanol, methyl-S-CoM, HS-CoM, HS-CoB and CoM-S-S-CoB in aqueous solution at 1 mol per kg and H_2 and methane in the gaseous state at 1 atm pressure). In turn, the ΔG^o for the CoM-S−S-CoB reduction reaction was calculated from the redox potential $E_o' = -140$ mV of the CoM-S−S-CoB/HS-CoM + HS-CoB couple.[80] Using these values, the free energy change associated with the MCR-catalyzed reaction is −33 kJ/mol. Before 2003, the redox potential of the CoM-S−S-CoB/HS-CoM + HS-CoB couple had been assumed to be near −200 mV, leading to a calculated free energy change of the MCR-catalyzed reaction of −45 kJ/mol.[144] From $\Delta G^o = -45$ kJ/mol, a $K_{eq} = k_{+1}/k_{-1}$ of almost 10^8 is calculated.

ΔG^o associated with ethane formation from ethanol and H_2 (−88.3 kJ/mol) is by 24 kJ/mol less exergonic than ΔG^o associated with methane formation from methanol and H_2 (−112.5 kJ/mol).[131] However, ΔG^o associated with ethane formation from ethyl-S-CoM and HS-CoB is not by 24 kJ/mol less exergonic than ΔG^o of methyl-S-CoM reduction to methane with HS-CoM ($\Delta G^o = -33$ kJ/mol) because ethyl-S-CoM formation from ethanol and HS-CoM is expected to be less exergonic than methyl-S-CoM formation from methanol and HS-CoM (how much was not found in the literature). Based on the bond strength difference H-CH_3 (438.9 kJ/ml) versus H-CH_2CH_3 (423.0 kJ/mol) the ΔG^o of ethane formation from ethyl-S-CoM and HS-CoB is estimated to be near −20 kJ/mol.

Reversible Inhibitors. Many MCR substrate analogues and homologues have been tested to probe the accessibility and reactivity of the Ni(I) in F-430 of MCR I.[91,119,133] Coenzyme M (app $K_i = 4$ mM), propyl-coenzyme M (app $K_i = 2$ mM), 2-azidoethane-coenzyme M (app $K_i = 1$ μM), and allyl-coenzyme M (app $K_i = 0.1$ mM) were found to be reversible inhibitors, inhibition being competitive to methyl-coenzyme M.[111,133] Reversible inhibition was also observed in the presence of diverse coenzyme B homologues and analogues.[119,134,135]

Irreversible Inhibitors. In 1978, 2-bromoethanesulfonate (BES) was found to be an effective inhibitor of methanogenesis,[139,140] which today is still widely used in ecological studies of the methane cycle. BES (app $K_i = 2$ μM) competes reversibly with methyl-coenzyme M in binding within the active site of MCR, but once it is bound, it alkylates the Ni(I) to a labile alkyl-Ni(III) derivative that collapses, yielding ethylene,[133,145,146] Also the inhibition of MCR with 3-bromopropanesulfonate (BPS) is irreversible. BPS (app $K_i = 0.1$ μM),[111] like BES, competes reversibly with methyl-coenzyme M in binding within the active site, but once it is bound, it alkylates the Ni(I) to a stable alkyl-Ni(III) derivative.[147,148] A stable alkyl-Ni(III) is also generated by brominated carboxylic acids with carbon chain length 5−16.[91] C_1- and C_2-polychlorinated hydrocarbons[149] are also irreversible inhibitors that all can easily enter the active site and oxidize the N(I) there.

An inhibitor used in ecological studies is 3-nitrooxypropanol (3-NOP) that oxidizes the N(I) in the MCR active site.[150] The nitroester is reduced by the Ni(I) in the active site of MCR to 1,3-propanediol and nitrite; the latter also reacts with Ni(I) in the active site, which is why 3-NOP is classified as a dual warhead inhibitor. 3-NOP is presently tested as an inhibitor of methanogenesis in the rumen of cattle and sheep.[151] 3-NOP has the advantage to not be charged and to thus be able to permeate into the methanogenic cells without requiring a transporter. E.g., in the case of BES, only those methanogens are sensitive to this inhibitor, which require coenzyme M as a vitamin and have a transport system for coenzyme M that also transports BES into the cells. Although BPS (app $K_i = 0.1$ μM) is a much better inhibitor of MCR than BES (app $K_i = 2$ μM) *in vitro*, it does not affect the enzyme *in vivo* because the coenzyme M transporter does not appear to transport BPS.

Whereas nitrite inactivates MCR at very low concentrations, nitrate is without any effect on MCR.[150] Nitrocompounds such as nitroethane, 2-nitroalcohol, and 2-nitro-L-propanol at mM concentrations inhibit methanogenesis *in vivo*,[152] whether they attack MCR is not known. There are a number of other compounds that inhibit methanogenesis at a low concentration *in vivo*, which might target MCR. Of these, ethylene (ethene) is the most interesting[153] because if the Ni(I) in MCR is able to add to the double bond of the alkene then this would be a sign of a strong one-electron reactivity of the Ni(I): Alkenes are known to react with free radicals and nucleophilic metals.[154]

Coenzyme B-Dependent Inactivation. The rate of inactivation by BES and BPS is stimulated by coenzyme B. At very low concentrations of BES, inactivation is dependent on the presence of coenzyme B. Also several fold stimulated by coenzyme B is the irreversible inhibition of MCR by cyano-coenzyme M, seleno-coenzyme M, and trifluoromethyl-coenzyme M.[133] These findings are of great importance for the catalytic mechanism because it shows that, upon coenzyme B binding, the nucleophilicity of Ni(I) in F-430 is considerably increased.

■ PROPOSED CATALYTIC MECHANISMS

Kinetic analyses revealed the two MCR isoenzymes from *M. marburgensis* to have a ternary complex kinetic mechanism (most probably an ordered bibi ternary complex mechanism) rather than a ping pong mechanism: Double reciprocal plots of initial rates versus the concentration of either one of the two substrates at different constant concentrations of the other substrate were linear and intersected on the abscissa to the left of the $1/v$ axis.[107] Thus, both substrates, methyl-coenzyme M and coenzyme B, have to bind after another to MCR before the first product, presumably methane, is released. From the MCR structure, it is not evident how methane gets out of or in the active site: a convincing gas channel has not been identified.

S_N2 Proposal. The mechanism long favored by the author of this Perspective assumed methyl-Ni(III)F-430 and methyl-Ni(II)F-430 as intermediates in the MCR catalytic cycle, the methyl-Ni(III) being formed by a nucleophilic attack by Ni(I) of the methyl group of methyl-coenzyme M in an S_N2 reaction.[117,118] The proposal was based on the finding that 2 mol pentamethylester of Ni(I)F-430 (Ni(I)F-430M) reacts

DOI: 10.1021/acs.biochem.9b00164
Biochemistry 2019, 58, 5198−5220

with 1 mol electrophilic methyl donors to 1 mol methane and 2 mol Ni(II)F-430 M[155] and that paramagnetic methyl-Ni(II)F-430 M can be trapped as likely an intermediate.[156] Ni(I)F-430 M is thus a nucleophile similar to cob(I)alamin with the difference that methyl-Ni(III)F-430 M is much easier to reduce to methyl-Ni(II)F-430 than methyl-cob(III)alamin to methyl-cob(II)alamin: the F-430-catalyzed reduction of methyl chloride with Ti(III) is almost 50 times more rapid than the cobalamin-catalyzed reaction and does not generate ethane as a side product.[157,158] The S_N2 proposal was also based on the property of cobalamin-dependent methionine synthase to catalyze the formation of methyl-cob(III)alamin from methionine, which is also a methylthioether ($\Delta G_0' = +30$ kJ/mol).[159,160] An important mechanistic argument was that both reactions proceed with inversion of stereoconfiguration of the methyl group[144]

Experimental support for the S_N2 mechanism came from the laboratory of Steven Ragsdale and of Evert Duin reporting that Ni(I)F-430 in MCR can be alkylated with methyl bromide or methyl iodide to methyl-Ni(III)F-430,[91,161] the structure of which was elucidated by X-ray absorption spectroscopy (XAS)[162] and X-ray structure analysis.[120] The methyl-nickel complex in MCR was found to react with coenzyme M to methyl-coenzyme M and, e.g., with CoB_8−SH, to Cob_8-S-CH_3, regenerating the MCR-red1 state[163] and with Ti(III) to methane and MCR-red1.[91,92] Observed radicals were interpreted to indicate that the methyl-Ni(III) bond is homolyzed, generating a methyl radical and Ni(II)F-430.[146] By transient kinetic methods, the decay of the active Ni(I) state coupled to the formation and subsequent decay of alkyl-Ni(III) and organic radical intermediates were observed at catalytically competent rates. These observations were considered to provide support for a MCR catalytic mechanism that involves methyl-Ni(III) and an organic radical as catalytic intermediates.[164]

However, the formation of the proposed methyl-Ni(III) intermediate from methyl-coenzyme M and MCR-red1 was never observed. This is in agreement with predictions from hybrid density function theory (DFT) computations performed in the laboratory of Per Siegbahn at the Stockholm University.[165−169] The computations predict that alkylation of the Ni(I)F-430 with the methyl thioether is too endergonic to allow the S_N2 reaction as part of the catalytic cycle. Also, a proposal involving protonation of the thioether's sulfur of the CH_3−S-CoM substrate, in analogy to cobalamin-dependent methyltransfer reactions, which should facilitate methyl-Ni(III)F-430 formation, was disfavored by DFT computations since the substrate has a much smaller proton affinity than the F-430 cofactor.[168]

Oxidative Addition Proposals. In collaboration with the group of Bernhard Jaun at the ETH Zürich, the Thauer laboratory could demonstrate that in 100% D_2O during methyl-coenzyme M reduction with coenzyme B to DCH_3 a significant amount of CH_2D−S-CoM was formed.[170,171] This finding allowed proposing that a σ-alkane-nickel complex could be formed by oxidative addition as an intermediate. However, based on DFT computations, this mechanism was predicted to be unfavorable for the MCR reaction, due to the large endothermicity for the formation of the ternary intermediate with side-on C−S (for CH_3−S-CoM) or CH (for methane) coordination of nickel.[168] In a different version of an oxidative addition mechanism,[172] the reaction is initiated by protonation of one of the ligands: nitrogen or Ni(I) in F-430. DFT computations indicated that also this mechanism is most probably energetically inaccessible for the MCR reaction.[168]

Siegbahn Proposal. On the basis of DFT computations using a truncated model of the active site derived from the crystal structure of the inactive Ni(II)MCR-ox1-silent form, the Siegbahn group proposed an alternative catalytic mechanism, in which the Ni(I) of F-430 in the active site attacks the thioether sulfur rather than the methyl group of coenzyme M, yielding coenzyme M with its thiolate sulfur bound to Ni(II)F-430 and a transient methyl radical that subsequently reacts with the thiol hydrogen of coenzyme B, generating methane and a coenzyme B thiyl radical (Figure 6).[165−167]

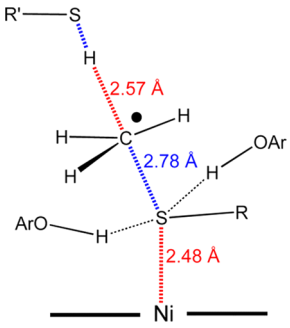

Figure 6. Transition state 1 according to the Siegbahn proposal.[167] Two bonds are broken (C−S and S−H, drawn blue), and two bonds are formed (Ni−S and C−H, drawn red) in a single step. F-430 is depicted as "Ni"; R mimics CoM, and R′ mimics CoB. OAr depicts phenol groups used in the model for the tyrosine residues. From Scheller et al., 2013.[16]

The group of Stephen Ragsdale recently provided experimental evidence for the transient methyl radical proposal by showing in single turnover experiments that the proposed high spin, EPR-silent Ni(II)thiolate is a kinetically competent intermediate.[136] Therefore, currently the "Siegbahn mechanism" appears to be the most acceptable one for MCR, which is why in the following this mechanism will be the basis for the discussion of the experimental results. Note that a catalytic mechanism cannot be proven but only disproven, and a mechanism has to explain all obtained experimental results, which at present the transient methyl radical proposal does not, as will be outlined in the next section.

■ INDIVIDUAL STEPS OF THE CATALYTIC CYCLE

The catalytic cycle begins with active MCR-red1a ("a" for absence of substrate) (Figure 7). Methyl-coenzyme M binds (step 1) followed by coenzyme B binding (step 2). The rate-determining endothermic step is most probably the reductive cleavage of the C−S bond of methyl-coenzyme M (step 3). In this first transition state, a planar methyl radical is positioned between the Ni(II) thiolate and the thiol hydrogen of coenzyme B, from which the methyl radical abstracts the hydrogen generating methane and a coenzyme B thiyl radical (step 4). Methane is assumed to be released in step 5 and the coenzyme thiyl radical reacts with the Ni(II) thiolate to generate the disulfide anion radical in an endothermic reaction (second transition state) (steps 5 and 6). Finally, the disulfide anion radical transfers its surplus electron to Ni(II) regenerating the Ni(I) oxidation state and forming CoM-S−S-CoB (step 7), which leaves the enzyme regenerating the

DOI: 10.1021/acs.biochem.9b00164
Biochemistry 2019, 58, 5198−5220

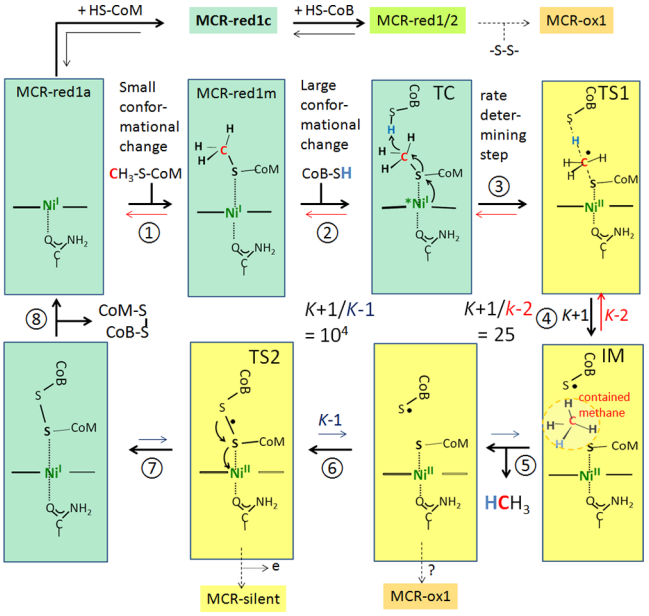

Figure 7. Schematic drawing of the catalytic cycle of methyl-coenzyme M reductase (MCR). The Ni(I) oxidation states are highlighted in greenish color, the Ni(II) oxidation states in yellow, and in the Ni(III) oxidation states in orange. TC, ternary complex. TS, transition state. IM, intermediate. *, increased reactivity of Ni(I)F-430 as a result of coenzyme B binding. k_{+1} = rate constant of the forward reaction (methane formation) (in black); k_{-1} = rate constant of the back reaction (methane oxidation) (in dark blue); k_{-2} = rate constant of the formation of CH_3−S-CoM from sterically contained methane (in red). The Ni(I) oxidation states exhibit characteristic EPR spectra: MCR-red1a, MCR in the absence of substrates; MCR-red1m, MCR in the presence of methyl-coenzyme M; MCR-red1c, MCR in the presence of coenzyme M; MCR-red1/2, MCR in the presence of coenzyme M and coenzyme B. In MCR-red1/2, part of the enzyme is in a Ni(III) hydride state (Figure 9). In the MCR-ox1 state, the thiol sulfur of coenzyme M is bound to the Ni(III) of F-430 (Figure 12). For details, see the text.

active enzyme without substrates bound (step 8). Note, it could also well be that methane is the last to leave having to wait until the heterodisulfide has diffused out making the way free.

Where indicated in Figure 7, MCR-red1c, MCR-silent, and MCR-ox1 branch off from the catalytic cycle. In the case of MCR-red1c, this is when the methanogenic cells are exposed to high H_2 and relatively low CO_2 concentrations (high intracellular HS-CoM and low CoM-S−S-CoB concentrations). In the case of MCR-silent and MCR-ox1, this is when the cells are exposed to low H_2 and relatively high CO_2 concentrations (low intracellular HS-CoM and high CoM-S−S-CoB concentrations).

Active and inactive MCR states in the catalytic cycle are based on steady state and presteady state kinetics, spectroscopic analyses, isotope effect measurements, and DFT computations. The EPR and isotope effect studies in the author's laboratory were performed in close collaboration with the groups of Bernhard Jaun at the ETH Zürich and Evert Duin, now at Auburn University, Alabama.

Active MCR without Substrates. The catalytic cycle starts with MCR without any substrates bound. The enzyme has a greenish color (λ_{max} = 385 nm) and exhibits an axial Ni(I)-derived EPR signal (g_1 = 2.252; g_2 = 2.070; g_3 = 2.061) designated as MCR-red1a ("a" for absent of substrates) derived from five coordinated Ni(I) in F-430 with an open upper nickel coordination site.[162,173] Double integration of the signal of the fully active enzyme revealed that both active sites contain F-430 in the reduced form, the spin concentration per Ni being in most cases approximately 0.9. The red1 signal shows a superhyperfine splitting due to the interaction of the electron of Ni(I) with the nuclear spin of the four nitrogens of the tetrapyrrolic ring system. The superhyperfine splitting is clearly resolved when the active enzyme is in the absence or presence of its substrates.[135] In fully active MCR (100 U/mg protein), the Ni(I) spin concentration is 1.0.[33]

Binding of the First Substrate. The first substrate to bind to MCR in the red1a state is methyl-coenzyme M (Figure 7, reaction 1). Binding results in the conversion of the Ni(I) EPR signal red1a into the EPR signal MCR-red1m ("m" for methyl-coenzyme M) (g_1 = 2.2515; g_2 = 2.0730; g_3 = 2.0635)[82] and in a small conformational change increasing the apparent affinity of the enzyme for its second substrate coenzyme B, thus guarantying that methyl-coenzyme M binds first. This was first deduced from structural studies indicating that binding of coenzyme M, an inhibitor competitive to methyl-coenzyme M, induces specific conformational changes ensuring that methyl-coenzyme M enters the substrate channel prior to coenzyme B as required by the active site geometry.[118] The Ragsdale laboratory could show that MCR can bind both substrates independently; however, only one binary complex, that with methyl-coenzyme M, is productive, while the one with coenzyme B is inhibitory: binding of methyl-coenzyme M to the inhibitory MCR-coenzyme B complex is highly disfavored (K_d = 56 mM) relative to the binding of coenzyme B to the productive MCR-methyl-coenzyme M complex (K_d = 79 μM).[174]

Using continuous-wave and pulse electron paramagnetic resonance spectroscopy in combination with selective isotope labeling (^{13}C and ^{2}H) of CH_3−S-CoM, it was shown that CH_3−S-CoM binds in the active site of MCR such that its thioether sulfur is weakly coordinated to the Ni(I) of F-430 with a long bond length near 3.94 Å.[175] The complex is stable until the second substrate, coenzyme B, binds. Results from EPR spectroscopy, along with quantum mechanical calculations, were used to characterize the electronic and geometric structure of the complex (Figure 8).[175]

In Figure 8, the S-methyl group of methyl-coenzyme M points away from the nickel and has a large degree of structural

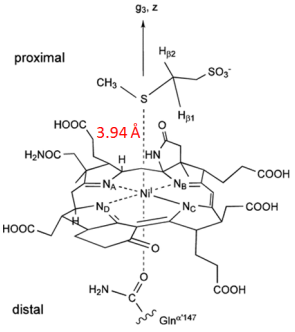

Figure 8. Electron nuclear double resonance (ENDOR) structure of methyl-coenzyme M bound to Ni(I) in the active site of methyl-coenzyme M reductase, exhibiting the EPR signal MCR-red1m. The Ni−S bond length is 3.94 Å, compared with a Ni−S bond length of 2.48 Å in the proposed transition state (Figure 6). From Hinderberger et al., 2008.[175]

DOI: 10.1021/acs.biochem.9b00164
Biochemistry 2019, 58, 5198−5220

freedom, which can be deduced from the observation of broad line widths in electron nuclear double resonance (ENDOR) spectra. In view of the indirect evidence for a major structural change in the active site upon the binding of HS-CoB (see below) and the substantial degree of freedom found for the S-methyl group, the question of the binding geometry of CH_3–S-CoM with respect to the nickel center in the transition state TS1 of the bond breaking step remains open. Interesting in this respect is that propyl-coenzyme M (app K_i = 2 mM) and allyl-coenzyme M (app K_i = 0.1 mM), which both inhibit MCR activity competitive to methyl-coenzyme M, induce the same red1 EPR signal as methyl-coenzyme M without being reduced.[133]

X-band hyperfine sublevel correlation (HYSCORE) spectra recorded at the echo maximum of the field-swept EPR spectrum for MCR-red1a and MCR-red1m revealed intense cross peaks at ca. 2.7 and 3.3 MHz and 3.3 and 2.7 MHz, representing the two double-quantum signals from a weakly coupled ^{14}N nucleus. The intense ^{14}N peaks were assigned to the NH_2 of the glutamine residue coordinate to the nickel ion from below via the oxygen (Figure 8).[175]

Binding of the Second Substrate. Coenzyme B can only effectively bind to MCR in the red1 state after methyl-coenzyme M is bound (reaction 2). How the enzyme can enforce a strictly ordered ternary complex mechanism[174] was described above. The reaction starts only when coenzyme B is added to the binary complex most probably because upon coenzyme B binding, via a conformational change in the nickel environment (see below), the nucleophilicity of the Ni(I) is increased such that it can react with methyl-coenzyme M. The latter is evidenced by the finding that the rate of Ni(I) quenching by 2-bromo-ethanesulfonate (BES) and other irreversible inhibitors (see above) is enhanced several fold upon addition of coenzyme B.[133] To indicate this, Ni(I) in the ternary complex in Figure 7 is drawn somewhat out of plane with an asterisk.

When the substrate analogue and competitive inhibitor coenzyme M rather than methyl-coenzyme M is bound to the active enzyme, which *in vivo* is the case when in the methanogenic cells the HS-CoM and HS-CoB concentrations are high and that of CoM-S–S-CoB is low, then there is a pronounced effect on the red signal that changes from MCR-red1c (g_1 = 2.2500; g_2 = 2.0710; g_3 = 2.0605)[82] to MCR-red1/2 (g_1 = 2.2880; g_2 = 2.2348; g_3 = 2.1790).[82] The red1c and red1/2 forms are not intermediates in the catalytic cycle but are enzymatically active forms because they react back to MCR-red1a as soon as coenzyme M is methylated to methyl-coenzyme M again.

The red1/2 signal is composed of 50% of the EPR signal MCR-red1cc (cc for coenzyme M and coenzyme B) and 50% of the two EPR species called MCR-red2a ("a" here for axial) and MCR-red2r (r for rhombic) (Figure 9).[83,170,176] The MCR-red1-type red1cc signal differs only slightly from the red1c signal. MCR-red2a has been assigned to a Ni(III) hydride complex,[170] or contrarily to a complex, in which the acidic CoM-SH proton is making a hydrogen bond to the Ni ion.[168] MCR-red2r has a Ni(I)-S coordination from HS-CoM, rhombic principal *g* values that are unusually high, and a very asymmetric spin density distribution on the four hydrpyrrolic nitrogens of the macrocycle F-430.[177,178]

The two MCR-red2 signals (Figure 9) can also be induced by the S-methyl- and the S-trifluoromethyl analogues of coenzyme B.[179] ^{19}F ENDOR data for MCR-red2a and MCR-red2r induced by S-CF_3-coenzyme B show that upon binding of the coenzyme B analogue, the end of the 7-thioheptanoyl chain of coenzyme B moves closer to the nickel center of F-430 by more than 2 Å as compared to its position in both the MCR-red1cc form[177,178] and the X-ray structure of the inactive Ni(II) MCR-ox1-silent form,[118] in which the sulfur of the heptanoyl arm of coenzyme B remains 8 Å from the nickel. This possible distance reduction of up to 2 Å was not captured in the DFT computations.[167,168]

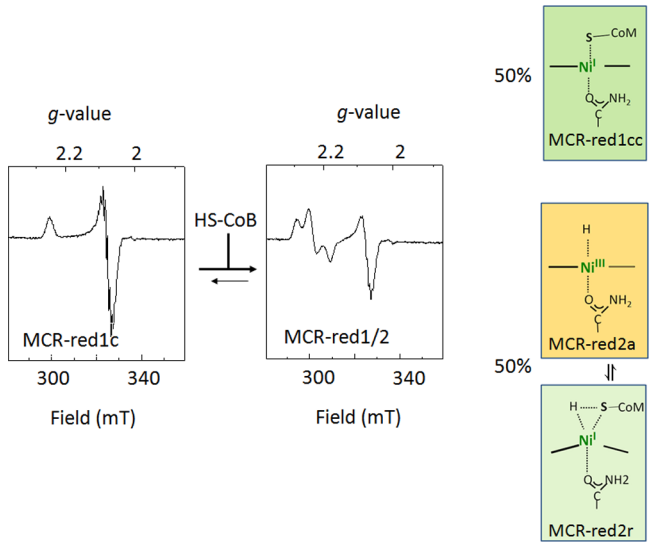

Figure 9. EPR spectra of methyl-coenzyme M reductase (MCR) with coenzyme M bound (MCR-red1c) and after additional binding of coenzyme B (MCR-red1/2). At saturating coenzyme B concentrations, the MCR-red1/2 spectrum is composed of 50% of the EPR spectrum MCR-red1cc, which is very similar to the EPR spectrum MCR-red1c and 50% of the MCR-red2, which in turn is composed of the axial MCR-red2a spectrum and the rhombic MCR-red2r spectrum. The active site nickel coordinations of MCR-red1cc, MCR-red2a, and MCR-red2r deduced from the spectra rather than the spectra are shown. Note that for MCR-red2a an alternative structure has been proposed, in which the acidic CoM-SH proton is making a hydrogen bond to the Ni ion.[168] The color of MCR in the red1/2 state is greenish orange and that of MCR in the red1 cm^3 state is greenish.[83,170,176] MCRs with nickel in the 3+ oxidation state have been shown to have a more orange than yellow color.[82] MCR-red2r is expected to have a greenish color similar to that of other MCRs with nickel in the 1+ oxidation state.

The finding that MCR-red1c is able to undergo such a large conformational change upon binding of coenzyme B can explain how binding of the second substrate can force methyl-coenzyme M and Ni(I) of the prosthetic group to interact in the ternary enzyme complex.[177,178,180] The results also help explain the dramatic change in the coordination environment induced in the transition from MCR-red1 to MCR-red2 forms (Figure 9) and opens the possibility that nickel 1+ coordination geometries other than square planar, tetragonal pyramidal, or elongated octahedral might occur in intermediates of the catalytic cycle.

Formation of the First Transition State. Based on hybrid DFT computations,[165−167] the Ni(I) in the ternary complex attacks the thioether sulfur of methyl-coenzyme M generating a transient methyl-radical and a high spin Ni(II) thiolate that is hydrogen bonded by the hydroxyl groups of two conserved tyrosines in the active site (shown in Figure 6 but not in Figure 7). A significant contribution to the transition

DOI: 10.1021/acs.biochem.9b00164
Biochemistry 2019, 58, 5198−5220

state is also the axial coordination of the rear glutamine oxygen ligand to nickel that is a permanent ligand but is assumed to coordinate more tightly in the Ni(II) and Ni(III) oxidation states.

At first sight, the modeling of a free methyl radical in the transition state did not appear to conform to the finding that ethyl-coenzyme M reduction to ethane proceeds with inversion of configuration of the ethyl group. However, the distance of the coenzyme B thiol hydrogen to the methyl carbon radical and the low energy barrier for H abstraction make a concerted mechanism possible so that the methyl radical has no time to rotate around its *y*-axis before abstracting the hydrogen from the thiol group of coenzyme B and by that generating the coenzyme B thiyl radical and methane (Figures 6 and 7).[165,166] The activation barrier for this first transition state (TS1) was calculated to be near 15 kcal/mol and for the second transition state (TS2) (see below) to be near 10 kcal/mol, considering entropy and dispersion.[167] The higher activation barrier for the first transition state implies that the first transition state is rate-limiting. The calculated transition state is supported by measured isotope effects using $^{13}CH_3$−S-CoM or CD_3−S-CoM as substrates.[16] The finding of a substantial $^{12}C/^{13}C$ isotope effect (1.04 ± 0.01) indicates that either cleavage of the C−S bond in methyl-coenzyme M or the formation of the C−H bond in methane occur in the rate-limiting step. The finding of an H/D secondary isotope effect of 1.19 ± 0.01 per D in the methyl group of CD_3−S-CoM indicates that it is the C−S bond cleavage that is the rate-limiting step because a larger H/D primary isotope effect would be expected if formation of the C−H bond was the main contributor of the $^{12}C/^{13}C$ isotope effect. A secondary isotope effect of 1.19 per D is consistent with a geometrical change of the methyl group from tetrahedral to trigonal planar upon going to the transition state of the rate-limiting step and with an almost free methyl radical in the highest transition state.[16] The secondary isotope effect appears not to be consistent with the formation of methyl-Ni(III) in the rate-determining step.[46]

The proposed transition state 1 (Figure 7) is also backed up by transient kinetic, spectroscopic, and computational approaches to study the reaction between active Ni(I) enzyme and its substrates by the Ragsdale group[136] as mentioned already above. Under single turnover conditions, CoM-S−Ni(II)F-430 was identified as an intermediate in the catalytic cycle when measured at 18 °C with CoB_6SH as an electron donor. The Ni(I) decay rate (0.35 s^{-1}) matched the methane formation rate determined with $^{14}CH_3$−S-CoM (0.31 s^{-1}) and the rate of CoM-S−Ni(II)F-430 formation (0.35 s^{-1}) determined via MCD. Only after more than 100 s, the spectrum of active MCR-red1 returned again.[136] Why it took so long still remains to be explained. Concomitant with the Ni(I) decay, the formation of low concentrations of various radicals was observed but none of these could be assigned to the coenzyme B thiyl radical.[40] However, thiyl radicals can have a broad EPR signal that can therefore easily be overlooked.[181]

Interesting for the catalytic mechanism of methyl-coenzyme M reduction is that trifluoromethyl-coenzyme M in contrast to difluoromethyl- and monofluoromethyl-coenzyme M is not a substrate of MCR; rather it is a coenzyme B-dependent irreversible inhibitor (app K_i = 6 mM).[133] "Differences in the S−C bond strength do not explain these results, since the DFT calculation shows that the S−C bond strengths are approximately equal for the different substrates. The major qualitative difference found between CHF_2−S-CoM and CF_3−S-CoM is the stereoinversion barrier. For CF_3, a stereoinversion barrier of 24.3 kcal/mol was obtained as compared to the value of only 6.1 kcal/mol for CHF_2. In the case of the natural substrate methyl-coenzyme M, the stereoinversion barrier is obviously equal to zero, since the methyl radical is planar".[165,166]

Sterically Contained Methane as an Intermediate. When methyl-coenzyme M reduction with coenzyme B is performed in 100% D_2O both DCH_3 and CH_2D−S-CoM are formed, the rate of the CH_3D formation (k_{+1}) (forward reaction 5) being 25 times more rapid than the rate (k_{-2}) of CH_2D−S-CoM formation (Figure 7; back reaction 4).[16,171] Since under the assay conditions the concentration of the product methane in solution was near zero, the rate of free DCH_3 oxidation to methyl-coenzyme M was essentially also zero. However, even when the methane concentration is allowed to build up, e.g., to 1 mM, the rate of methane formation from methyl-coenzyme M (k_{+1}) is 10^4 times more rapid than the rate of free methane oxidation to methyl-coenzyme M (k_{-1}). The rate (k_{-2}) of CH_2D−S-CoM formation in D_2O from CH_3−S-CoM thus indicates that the methane generated after the first transition state is sterically hindered from leaving the active site and can thus react backward.[16,171] This is even more pronounced when ethane is formed from ethyl-coenzyme M in D_2O. In this case, the k_{+1} to k_{-2} ratio was found to be 1:100, indicating that ethane was almost completely trapped within the active site. Labeling with deuterium of ethyl-coenzyme M during MCR-mediated reduction to ethane in D_2O was both in the α- and β-positions. This indicates that the trapped ethane was able to freely rotate in all directions before reacting back to ethyl-coenzyme M.[138,171]

As mentioned above, binding of propyl-coenzyme M and of allyl-coenzyme M to active MCR induces an identical change in the MCR-red1a EPR spectrum as methyl-coenzyme M despite the fact that the methyl-coenzyme M analogues are not noticeably reduced to propane and propene, respectively. When propyl- and allyl-coenzyme M conversion with coenzyme B was tested in D_2O, no deuterium exchange into the propyl and allyl group was observed,[16,138] indicating that propane or propene were not formed because they were trapped in the active site. The propyl and allyl radicals are much more stable than the methyl radical. The lack of exchange of deuterium into the propyl group of propyl-coenzyme M is of interest with respect to the observation that in some archaea MCR appears to be involved in the anaerobic oxidation of propane.[54]

An alternative mechanism to explain the deuterium exchange into the methyl group of coenzyme M is that methane binds to nickel as a σ-complex[171] (Figure 10). Between the two mechanisms (methane physically prevented from leaving the active site for steric reasons versus methane covalently bound to nickel as a σ-complex) cannot be decided because the second transition state (TS2) is lower in energy and thus cannot be probed by kinetic isotope effects.[16] Although DFT calculations have made this oxidative addition mechanism unlikely,[168] it should not be completely excluded until it is understood what "sterically contained CH_4" really is and how the measured primary and secondary kinetic isotope effects possibly affect the outcome of the DFT computations.[168] Also, the exact determination of the solvent kinetic isotope effect (H_2O/D_2O) is awaited (see below).

DOI: 10.1021/acs.biochem.9b00164
Biochemistry 2019, 58, 5198−5220

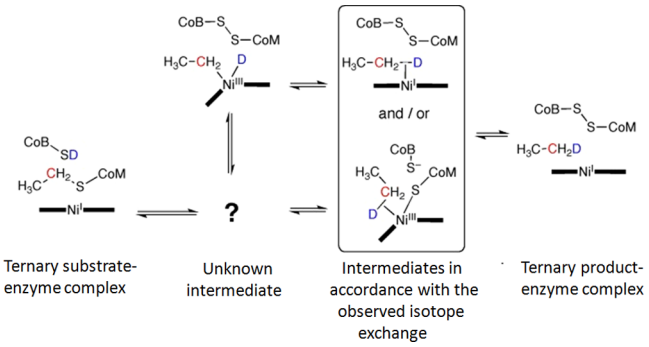

Figure 10. Isotopic exchange of deuterium from D_2O into the methyl group of methyl-coenzyme M, consistent with formation of a σ-alkane-nickel complex as an intermediate. For clarity, the intermediates are drawn with the non-natural substrate ethyl-coenzyme M labeled with one ^{13}C (drawn in red) in a deuterated medium. The ligand of coenzyme F-430 is shown schematically as bold lines. The bend in the Ni(III) intermediate symbolizes two cis coordination sites and a distorted equatorial macrocycle. The legend and figure are from Scheller et al., 2010 (reproduced with permission of Wiley-VCH Verlag GmbH & Co. KG).[171] (See also refs 16 and 138).

Formation of the Second Transition State. Methane formation catalyzed by MCR involves at least one intermediate (sterically contained methane or possibly σ-complex) and thus two transition states (Figure 7). Partitioning of the intermediate between the forward reaction and the reversal to methyl-coenzyme M is temperature-dependent with the highest forward commitment (25:1) found at a temperature of 60 °C. The commitment at 4 °C was 1.1 to 1. The temperature dependence in itself constitutes independent evidence for at least two transition states.[16] From the 25:1 ratio, the second transition state is predicted to lie at 60 °C about 10 kJ/mol lower in energy than the first one. To the contrary, in ethane formation from ethyl-coenzyme M, it is the second transition state that was found to be energetically higher by more than 10 kJ/mol at 60 °C.[138,171] As indicated above the activation barrier obtained from DFT for TS1 was near 15 kcal/mol (near 60 kJ/mol) and for TS2 it was near 10 kcal/mol (near 40 kJ/mol). Transition state 2 is therefore calculated to lie 20 kJ/mol lower than transition state 1.[167] From the observed deuterium-labeling rates of methyl-coenzyme M and methane, when the reaction was performed in D_2O, the difference between the two transition states was calculated to be only about 10 kJ/mol.[16] The two methods thus yielded significantly different results, which is not surprising since the DFT calculations did not consider conformational changes and the existence of the sterically contained methane as an intermediate. Also, potentially valuable quantum mechanical calculations of the isotope effect, although important, are still missing.[168]

In transition state II, the heterodisulfide anion radical is in complex with Ni(II)F-430. Disulfide anion radicals have redox potentials more negative than −1 V,[182] enabling the disulfide anion radical to transfer its electron to Ni(II)F-430 with a redox potential more negative than −600 mV.

Enzyme Product Complex. The Ni(I) CoM-S−S-CoB complex is not very stable[113] probably because it is in equilibrium with the Ni(II) CoM-S−S-CoB radical anion complex (transition state II) (Figure 7), when the product CoM-S−S-CoB builds up. The disulfide anion radical is, because of its negative one-electron redox potential below −1 V,[182] even more sensitive to oxidation than Ni(I) in Mcr-red1, oxidation yielding inactive MCR-silent with the structure shown in Figure 5B. Thus, when *M. marburgensis* growing on 80% H_2 and 20% CO_2 is harvested, the cells contain almost only MCR-silent because the low amount of H_2 dissolved in the medium (<0.2 μmol/mL) is consumed within minutes after gassing has ceased, resulting in an intracellular increase in CoM-S−S-CoB that is no longer reduced (see Figure 3). The electron acceptor for the one-electron oxidation reaction is not yet known.

When cells are gassed with 80% N_2 and 20% CO_2 before the harvest, which removes all of the H_2 within seconds and which induces the formation of MCR-ox1,[79] then the increased intracellular CoM-S−S-CoB concentration probably pushes the back reaction beyond transition state II (Figure 7). This would allow the coenzyme B thiyl radical (near 0 V),[182] in the absence of methane, to slowly extract an electron from CoM−S-Ni(II)F-430, generating coenzyme B and MCR-ox1, in which $^-$S-CoM is bound via its thiolate sulfur to Ni(III)F-430. The structure of MCR-ox1 has been determined by NMR and XAS measurements to be very similar to that of CoM-S Ni(II) shown in Figure 5A.[90]

In vivo the MCR-ox1 signal can also be induced by the addition to cultures of *M. marburgensis* of sodium sulfide (20 mmol/L), which at this concentration completely inhibits methanogenesis.[86] *In vitro* MCR-ox1 was found to be formed from MCR-red1/2 upon polysulfide addition[82] rather than by sulfide. Both findings can be explained assuming that a coenzyme M persulfide is formed[183] from either coenzyme M and polysulfide or CoM-S−S-CoB and sulfide. In the presence of coenzyme B, the persulfide would react with Ni(I)F-430 to S^--Ni(III) + HS-CoM and/or CoM−S-Ni(III) + H_2S. The finding that ^{35}S was incorporated from sulfide into MCR-ox1 and released again upon reduction to Ni(I)F-430 supports this possibility.[86]

The formation of inactive MCR-silent and MCR-ox1 (Figure 7), when within methanogenic cells the CoM-S−S-CoB concentration builds up, leads to an inactivation of the enzyme under conditions, where electrons are not available for CO_2 reduction. When more electrons become available again, then the inactive MCR is ready[86] to be reduced to the active form in an ATP-dependent reaction (see the Reactivation of Inactive MCR section).

Methane Oxidation to Methyl-Coenzyme M. According to the principle of microscopic reversibility, the reaction mechanism is identical in both directions of the catalyzed reaction.[46,167] Because the equilibrium of the MCR-catalyzed reaction is on the methane side under standard conditions (ΔG° = −30 kJ/mol for methane formation), MCR is predicted to catalyze the back reaction at only a very low specific activity (see the Catalytic Properties section). Indeed, methane oxidation to methyl-coenzyme M in H_2O as catalyzed by MCR-red1from *M. marburgensis* proceeds at a specific rate of only about 0.01% of the specific rate of methyl-coenzyme M reduction to methane (100 μmol min^{-1} mg $protein^{-1}$). The initial rate of methane oxidation at 1 bar CH_4 and 60 °C was found to be 11.4 nmol min^{-1} mg $protein^{-1}$.[36] The ratio of the back reaction to the forward reaction (100 μmol min^{-1} mg $protein^{-1}$) is thus near 10^{-4} ($V_{-1}/V_{+1} = 10^{-4}$) (Figure 7).

As already mentioned, when methane oxidation to methyl-coenzyme M was measured in 100% D_2O, only CH_3−S-CoM was formed, indicating the absence of H/D exchange from the

DOI: 10.1021/acs.biochem.9b00164
Biochemistry 2019, 58, 5198−5220

medium into the ternary complexes (see the legend in Figure 1). This made it possible to study isotope effects for methane activation because the methyl-coenzyme M formed from methane does not undergo isotopic exchange and can therefore be analyzed in order to determine isotope effects. Methane activation was found to proceed with a primary isotope effect of 2.44 ± 0.22 for the C−H versus the C−D bond breakage and with a secondary isotope effect corresponding to 1.17 ± 0.05 per D.[16] The primary isotope effect is quite significant, reflecting that in the methane activating direction a thiyl radical abstracts a hydrogen atom from methane, which is a very endothermal reaction ($\Delta H^{\circ} \approx 70$ kJ/mol) and which is not observed in nonenzymatic reactions because follow-up reactions of the thiyl radicals such as dimerization are much faster in solution. However, in the active site of MCR, a thiyl radical might persist for the time needed to react with methane.[16] The secondary isotope effect on methane activation (1.17 ± 0.05 per D) is compatible with methyl radical formation from methane (respectively, a methyl radical-like transition state).[16,167]

Alkane oxidation via an attack of the alkane by a thiyl radical, as proposed for MCR-catalyzed methane oxidation (Figure 7), is unprecedented in organic chemistry but not in biochemistry.[53,184] In organic chemistry, anoxic alkane C−H bond activation is generally achieved by interaction of the alkane with a transition metal center (e.g., ref 185). As indicated above, the involvement of a σ-alkane-nickel complex as an intermediate in methane oxidation to methyl-coenzyme M[171] cannot yet be completely ruled out. This and other mechanisms of methane oxidation catalyzed by MCR involving organometallic intermediates have been reviewed by Scheller et al., 2017.[46]

SOLVENT KINETIC ISOTOPE EFFECT (H_2O/D_2O), PROTON INVENTORY STUDIES, AND CLUMPED ISOTOPOLOGUES

Solvent Kinetic Isotope Effect. In 100% D_2O, CH_3−S-CoM was reduced to DCH_3 with low amounts of D_2CH_2 accumulating at the end. The apparent K_M and apparent V_{max} were only slightly different from those determined in 100% H_2O. From the differences, a primary solvent kinetic isotope effect (KIE) between 1 and 1.6 was estimated. The reason for the large error bar is that determinations of k_{cat} over K_M with the assay employed (discontinuous measurement of methane via gas chromatography; low enzyme concentration) is not very precise, considering that even traces of O_2 negatively affect k_{cat} of MCR.[16]

Proton Inventory Studies. In the case of the MCR-catalyzed reaction, a proton or deuterium ends up in the product dependent on whether the reaction is performed in H_2O or D_2O (Figure 1). Therefore, the isotope distribution in the product (CH_4 versus CH_3D) can be studied as the function of the deuterium content of water (proton inventory technique),[186] yielding the apparent fractionation factor Φ_{app} that is a composite of the equilibrium fractionation factor Φ of the hydrogen-donating group before the rate-limiting step and the solvent kinetic isotope effect KIE = Φ/Φ_{app}. The equilibrium fractionation factor Φ for HS-CoB in distilled water at 25 °C was determined by NMR spectroscopy to be 0.42, increasing somewhat (7%) between 4 and 50 °C.[187] The apparent fractionation factor Φ_{app} for methane formation from methyl-coenzyme M was found to be 0.27 (Figure 11, red curve). From $\Phi_{HS\text{-}CoB} = 0.42$ and $\Phi_{app} = 0.27$, a solvent KIE = 1.55 is calculated, which is within the range of the solvent KIE estimated to lie between 1.0 and 1.6 from k_{cat}/K_M measurements. The proton inventory study is thus consistent with coenzyme B being the hydrogen-donating group before the rate-limiting step as assumed in Figure 7. If, for example, the OH groups ($\Phi = 1.0$) of the two conserved tyrosines in the active site would be the hydrogen donor before the rate-limiting step, then the solvent KIE effect would have to be 3.7, which clearly was not found.

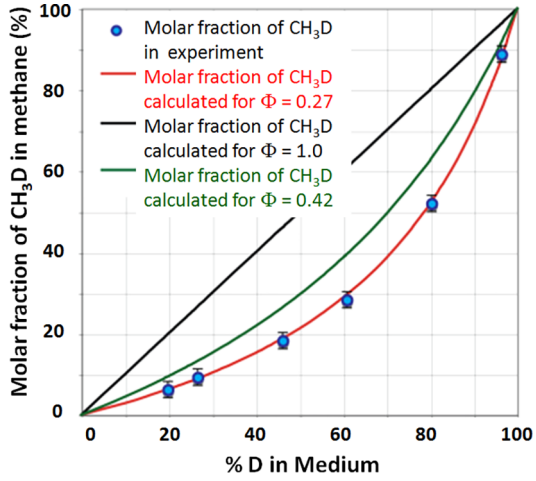

Figure 11. Proton inventory for methyl-coenzyme M reduction with coenzyme B to methane in H_2O/D_2O containing increasing amounts of deuterium as catalyzed by MCR I of *M. marburgensis*. The reaction was performed in the presence of Ti(III) and traces of cob(II)alamin to regenerate coenzyme B from CoM-S−S-CoB. The figure was taken with permission from the Ph.D. Thesis of S. Scheller[188] (Figure 4) and slightly modified. When coenzyme B was limiting (not regenerated by reduction of CoM-S−S-CoB), then the apparent fractionation factor was found to be 0.297.[188]

However, one has to consider that the solvent KIE is near 1.0 rather than near 1.6, which would also be in the range determined experimentally. In this case, the found apparent fractionation factor of 0.27 is only explainable if the group providing the hydrogen in the rate-limiting step has an equilibrium fractionation factor smaller than 0.3, which would exclude coenzyme B with $\Phi = 0.42$ as being the hydrogen-donating group before the rate-limiting step (KIE = Φ/Φ_{app}). Metal hydrides such as $CpW(CO)_2(PMe_3)H$ can have equilibrium fractionation factors as small as 0.2.[189,190] A solvent kinetic isotope effect near 1 would thus favor a Ni hydride as an intermediate (Figure 10) and exclude coenzyme B as the hydrogen-donating group before the rate-limiting step as assumed in Figure 7. It will therefore be of utmost importance in future studies to determine the solvent kinetic isotope effect of methane formation from methyl-coenzyme M with a higher accuracy than was until now possible.

There is one conclusion from the proton inventory results that appears to be straightforward: the results are not in favor of the formation of a methyl-Ni(III) intermediate in the rate-limiting step because the hydrogen-donating group would provide the hydrogen after the rate-limiting step, resulting in an apparent fractionation factor of 1, which was definitely not found. Both in the case of NH and OH groups, $\Phi = 1$.

Clumped Isotopologues. Measurements of clumped isotopologues of methane ($^{13}CH_3D$ and/or $^{12}CH_2D_2$) are being applied as tools to constrain the source of methane in a variety of environments.[191,192] $\Delta^{13}CH_3D$ values are a

DOI: 10.1021/acs.biochem.9b00164
Biochemistry 2019, 58, 5198−5220

composite of temperature-dependent equilibrium isotope effects and nonequilibrium kinetic isotope effects. Low $\Delta^{13}CH_3D$ values characteristic for methanogens growing under laboratory conditions have been suggested to be produced during enzymatic reactions common in all methanogenic pathways, such as the reduction of methyl-coenzyme M.[193] Determination of $\Delta^{13}CH_3D$ with purified MCR could not only help interpret the *in vivo* results but also contribute to the understanding of the catalytic MCR mechanism.

HALF-OF-THE-SITES REACTIVITY

As mentioned above, when MCR I from in the red1a state is supplemented with coenzyme M and coenzyme B, the axial red1c EPR signal is partially converted into the rhombic MCR-red2r and axial MCR-red2a signals (Figure 9). The conversion is in a temperature-dependent equilibrium. The equilibrium constant (K_{eq} = [MCR-red2]/[MCR-red1]) was 0.1 at 0 °C and increased to approximately 1 at 20 °C. Above 20 °C, K_{eq} remained constant. This was shown both by EPR spectroscopy and by UV−vis spectroscopy.[135] Thermodynamics predict for an endothermic reaction that the equilibrium constant increases with temperature until $K_{eq} = \infty$. The finding that the increase in MCR-red2 with an increasing temperature leveled off, when approximately 50% of the red1 signal present initially was converted to the red2 signals (K_{eq} = 1), was therefore unexpected. It can be explained, however, considering that each MCR molecule harbors two structurally interacting active sites and postulating that in the presence of coenzyme M and coenzyme B only one of the two active sites can be converted from the MCR-red1 state into the two MCR-red2 states. The temperature dependence thus indicates that in the presence of coenzyme M and coenzyme B the two active sites in one MCR molecule are in two different states, suggesting that active MCR shows half-of-the sites reactivity.[135]

The reduction of methyl-coenzyme M with coenzyme B catalyzed by MCR takes place in a hydrophobic pocket, from which water is excluded. The two substrates thus have to be stripped of water when entering the active site, and after reaction, the product CoM-S−S-CoB has to be expelled into the water phase. This is most probably achieved by a conformational change, which is driven by one of the exergonic steps in the catalytic cycle. The two active sites could operate independently or coupled. The finding of half-of-the-sites reactivity for MCR is in favor of the two active sites being coupled. The intertwined hexameric structure of MCR, in which the lower axial ligand to nickel in the one active site is provided by the glutamine of the α subunits that mainly forms the other active site and, *vice versa*, is optimally suited for such a mechanism, considering also that the lower axial acylamide ligand to nickel oscillates between loosely bound N(I) states and tightly bound N(II) states during the catalytic cycle (Figure 7). Thus, coupling of the endergonic and the exergonic steps of the catalytic cycle in the two active sites could be envisioned as a strategy employed by MCR to lower the activation energy of the rate-limiting step in analogy to dual stroke motors.[135]

The active site thioglycine in the α subunit (McrA) has been considered to be involved in the half-of-the-sites reactivity because the thioglycine peptide bond facilitates a cis−trans isomerization of the peptide bond, connecting the thioglycine to the next amino acid.[135] Exchange of the thioglycine to glycine yielded an MCR that was still active as deduced from the fact that the mutated cells grew normally when not stressed.[127] Whether the variant enzyme still shows full activity cannot be deduced from this *in vivo* experiment as has been outlined above (see the Post-Translational Modifications).

ATP-DEPENDENT REDUCTIVE REACTIVATION OF MCR

When the nickel in MCR gets oxidized to Ni(II), either as the result of a high intracellular CoM-S−S-CoB/HS-CoM + HS-CoB ratio or by, for example, O_2 or chloroform,[149] the enzyme is inactivated but can be reactivated again in an ATP-dependent enzyme-catalyzed reaction. In 1976, it was reported that three components, A, B, and C, of *Methanobacterium* cell extracts and ATP are required for methyl-coenzyme M reduction with H_2 to methane.[4,5] Component A of the MCR system was later resolved into three protein fractions, A1, A2, and A3; the presence of all three of which was required besides coenzyme B (component B) and catalytic amounts of ATP for MCR (component C) to catalyze methyl-coenzyme M reduction with H_2 to methane.[194−196] Component A3 was finally resolved into two components, A3a and A3b. Only components A2 and A3a, coenzyme B, MCR, and ATP were required when T(III) rather than H_2 was the electron donor.[197] A2 was found to be an ATP-binding protein[198] and A3a to be an iron−sulfur protein.[197] Based on these studies, it was proposed in 1988 that the function of A2 and A3a is to catalyze the reduction of nickel in F-430 of MCR from the inactive Ni(II) to the active Ni(I) oxidation state in an ATP-dependent reaction.[199] All of these activation studies were hampered by the fact that only specific activities of MCR of about 0.1 μmol min^{-1} mg protein^{-1} were maximally reached.

A breakthrough came from the finding that activated MCR is instable in the presence of its product CoM-S−S-CoB[113] (see the Enzyme Product Complex section). Taking this into account, inactive MCR-silent or MCR-ox1 were incubated in the presence of A2, A3a, ATP, and dithiothreitol as an electron donor in the absence of methyl-coenzyme M and coenzyme B that upon MCR activation would be converted to CoM-S−S-CoB. Under these conditions, MCR-ox1 was activated to 100% and MCR-silent to 65% as revealed by EPR spectroscopy (Figure 12).

The colorless A2 protein has a molecular mass of near 60 kDa and possesses two ATP-binding domains.[198] A2 appears to be specific for the MCR of the methanogen, in which it is synthesized. In *M. marburgensis*, there is only one gene for A2 although the organism contains two MCR isoenzymes. In other methanogens, there can be two copies of the A2 gene and only one set of genes for MCR. The brown A3a protein is a nonhomogeneous 700 kDa multienzyme complex that includes the *mcrC* gene product (see the Subunit Composition section), an Fe-protein homologue, an iron−sulfur flavoprotein, polyferredoxin, acetyl-CoA synthase/decarbonylase, and protein components involved in heterodisulfide reductase coupled electron bifurcation.[113] The details still have to be worked out.

Recently it was found that inactive MCR in cells of *M. marburgensis* is fully activated when the cells are incubated in the presence of CO, which in the cells is oxidized to CO_2 with ferredoxin as an electron acceptor in a carbon monoxide dehydrogenase-catalyzed reaction.[200] Partial activation (to 50 nmol min^{-1} mg protein^{-1} ≙ 0.05%) of purified MCR from *Methanosarcina thermophila* by CO in a ferredoxin- and carbon

DOI: 10.1021/acs.biochem.9b00164
Biochemistry 2019, 58, 5198−5220

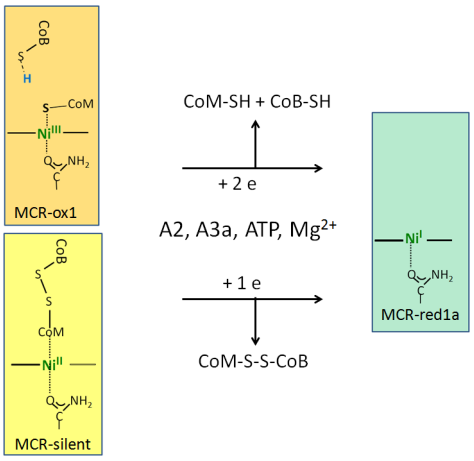

Figure 12. Reductive activation of inactive MCR-silent and MCR-ox1 to MCR-red1a. The active site nickel coordination deduced from the EPR spectra is shown. For coordination of CoM-S−S-CoB via the sulfonate group of CoM-SH in MCR-silent, see Figure 5B. A2 is a 60 kDa protein with two ATP-binding sites and A3a a 700 kDa nonhomogeneous iron−sulfur flavoprotein complex composed of several different proteins. The electrons can be provided by dithiothreitol.

monoxide dehydrogenase-dependent reaction had previously been reported.[114] Incubation of the *M. marburgensis* cells with H_2 ($E_o' = -414$ mV) also yielded an active enzyme but much more slowly than with CO ($E_o' = -520$ mV) in agreement with the assumption that the reduction of the nickel in MCR ($E_o' = \leftarrow 600$ mV) with CO at high concentrations is thermodynamically possible but not with H_2. The reduction of the Ni in MCR by H_2 becomes exergonic only when coupled to the hydrolysis of ATP.

In hydrogenotrophic methanogens, 0.5 mol ATP is formed per mol CO_2 reduced to methane (Figure 4).[42] If MCR has to be reactivated, let us say after 100 turnovers, and if for the reactivation 1 ATP is required, then the ATP gain is predicted to decrease from 0.5 mol ATP/mol methane to 0.49 mol ATP/mol methane. Such a decrease in growth yield makes the methanogens not less viable.[74] However, without the reactivation mechanism, these microorganisms would not be able to recover from conditions not favorable for methyl-coenzyme M reductase and methanogenesis.

Light-Dependent Activation of MCR. In 1991, it was shown by Olson and Wolfe[201] that inactive purified MCR was partially activated by exposure to light above 400 nm. Components necessary for light activation and methanogenesis were coenzyme B, methyl-coenzyme M, and titanium(III) citrate rather than ATP, A2, and A3. Photoactivation was suppressed by inhibitors of methanogenesis such as 2-bromoethanesulfonate, CoB_6−SH, and dithionite. Although the specific activity was very low (35 nmol of CH_4 per h per mg of protein), the experiments clearly showed that there is a light-sensitive component involved in the activation of MCR.

CONCLUSION AND OUTLOOK

MCR was discovered almost 50 years ago in methanogens and has been intensively studied ever since then. In the beginning of the 2000s, MCR was also found in methane-oxidizing anaerobic archaea.[37,38] Recent reports indicate that MCR may be also involved in anaerobic butane oxidation[54] and in anaerobic ethane oxidation,[55] as evidenced by the finding of MCR and butyl-S-CoM or ethyl-S-CoM in the respective archaea. Butane-oxidizing archaea did not oxidize methane or ethane, and ethane-oxidizing archaea did not oxidize methane or butane, which, based on the crystal structure and substrate specificity of MCR from methanogenic archaea, is very surprising. How these alkyl-coenzyme M reductases can prevent methane from being oxidized to methyl-coenzyme M and methyl-coenzyme M from being reduced to methane is not understood. The catalytic mechanism proposed for MCR from methanogens in Figure 7 postulates a "sterically contained methane" as an intermediate in order to explain the incorporation of deuterium into the methyl group of methyl-coenzyme M when MCR catalyzes methane formation from methyl-coenzyme M in D_2O. The exchange is also consistent with a σ-alkane-nickel complex as an intermediate but formation of such a σ-complex is not favored by DFT calculations. When MCR I from *M. marburgensis* catalyzes ethane formation from ethyl-coenzyme M in D_2O, the exchange rate of deuterium into the ethyl group even exceeds the rate of ethane formation.[138,171] There thus appears to be a yet unknown gate that determines substrate specificity. The described catalytic mechanism also cannot explain, why the two active sites of the $\alpha_2\beta_2\gamma_2$ hexamer are not only structurally but also mechanistically coupled (half-of-the-sites reactivity).[135] It appears from mutation studies published in the last two years that the unique, highly conserved post-translational modifications, thioglycine and 5-methylarginine, in the active site of MCRs are essential only under stress conditions.[127,130] One of the assumptions made in the interpretation of the *in vivo* genetic results is that MCR catalyzes the growth-rate-limiting step, which is only correct under growth conditions prevailing in the natural environment of the methanogens. Under batch culture laboratory conditions, frequently, the rate of anabolism rather than that of catabolism limits growth rate. Measurements of the catalytic efficiency (k_{cat}/K_M) and of the activation energy of the mutated MCR are therefore required to elucidate the function of the post-translational modifications. The 700 kDa enzyme complex A3a that catalyzes together with the chaperone A2, the ATP-dependent reduction of inactive MCR, to active enzyme has not yet been characterized.[113] The ATP costs of MCR reactivation during growth are not known. In conclusion, there is still a lot to be resolved before we start understanding how MCR and its activation function.

AUTHOR INFORMATION

Corresponding Author

*E-mail: Thauer@mpi-marburg.mpg.de.

ORCID

Rudolf K. Thauer: 0000-0003-0714-0148

Funding

The author has been without funding since the end of 2014, when he retired.

Notes

The author declares no competing financial interest.

ACKNOWLEDGMENTS

The author thanks Dr. Seigo Shima, Max Planck Institute in Marburg, for helpful suggestions.

DOI: 10.1021/acs.biochem.9b00164
Biochemistry 2019, 58, 5198−5220

■ ABBREVIATIONS

ANME, anaerobic methane oxidizers; AOM, anaerobic oxidation of methane; DFT, density function theory; ENDOR, electron nuclear double resonance; EPR, electron paramagnetic resonance; GPP, gross primary production; HS-CoM, coenzyme M; HS-CoB, coenzyme B; HYSCORE, hyper fine sublevel correlation; MCR, methyl-coenzyme M reductase

■ REFERENCES

(1) Mcbride, B. C., and Wolfe, R. S. (1971) New coenzyme of methyl transfer, coenzyme M. *Biochemistry 10*, 2317−2324.

(2) Taylor, C. D., and Wolfe, R. S. (1974) Structure and methylation of coenzyme M ($HSCH_2CH_2SO_3$). *J. Biol. Chem. 249*, 4879−4885.

(3) Shapiro, S., and Wolfe, R. S. (1980) Methyl-coenzyme-M, an intermediate in methanogenic dissimilation of C-1 compounds by *Methanosarcina barkeri*. *J. Bacteriol. 141*, 728−734.

(4) Gunsalus, R. P., and Wolfe, R. S. (1976) Components and cofactors for enzymatic formation of methane from methyl-coenzyme-M. *Fed Proc. 35*, 1547−1547.

(5) Gunsalus, R. P., and Wolfe, R. S. (1980) Methyl coenzyme-M reductase from *Methanobacterium thermoautotrophicum* - Resolution and properties of the components. *J. Biol. Chem. 255*, 1891−1895.

(6) Ellefson, W. L., and Wolfe, R. S. (1980) Properties of component C of the 2-(methylthio)Ethanesulfonate (CH_3−S-CoM) methylreductase of *Methanobacterium*. *Fed Proc. 39*, 1773−1773.

(7) Ellefson, W. L., and Wolfe, R. S. (1981) Component-C of the methylreductase system of *Methanobacterium*. *J. Biol. Chem. 256*, 4259−4262.

(8) Ankel-Fuchs, D., and Thauer, R. K. (1986) Methane formation from methyl-coenzyme-M in a system containing methyl-coenzyme-M reductase, component-B and reduced cobalamin. *Eur. J. Biochem. 156*, 171−177.

(9) Noll, K. M., Rinehart, K. L., Tanner, R. S., and Wolfe, R. S. (1986) Structure of component-B (7-mercaptoheptanoylthreonine phosphate) of the methylcoenzyme-M methylreductase system of *Methanobacterium thermoautotrophicum*. *Proc. Natl. Acad. Sci. U. S. A. 83*, 4238−4242.

(10) Clements, A. P., White, R. H., and Ferry, J. G. (1993) Structural characterization and physiological-function of component-B from *Methanosarcina-thermophila*. *Arch. Microbiol. 159*, 296−300.

(11) Ellermann, J., Hedderich, R., Bocher, R., and Thauer, R. K. (1988) The final step in methane formation - investigations with highly purified methyl-CoM reductase (Component-C) from *Methanobacterium-thermoautotrophicum* (Strain Marburg). *Eur. J. Biochem. 172*, 669−677.

(12) Bobik, T. A., Olson, K. D., Noll, K. M., and Wolfe, R. S. (1987) Evidence that the heterodisulfide of coenzyme-M and 7-mercapto-heptanoylthreonine phosphate Is a product of the methylreductase reaction in *Methanobacterium*. *Biochem. Biophys. Res. Commun. 149*, 455−460.

(13) Hedderich, R., Berkessel, A., and Thauer, R. K. (1989) Catalytic properties of the heterodisulfide reductase involved in the final step of methanogenesis. *FEBS Lett. 255*, 67−71.

(14) Kaster, A. K., Goenrich, M., Seedorf, H., Liesegang, H., Wollherr, A., Gottschalk, G., and Thauer, R. K. (2011) More than 200 genes required for methane formation from H_2 and CO_2 and energy conservation are present in *Methanothermobacter marburgensis* and *Methanothermobacter thermautotrophicus*. *Archaea 2011*, 1.

(15) Jaun, B. (1993) Methane d formation by methanogenic bacteria - redox chemistry of coenzyme F430. *Met Ions Biol. Syst 29*, 287−337.

(16) Scheller, S., Goenrich, M., Thauer, R. K., and Jaun, B. (2013) Methyl-coenzyme M reductase from methanogenic Archaea: Isotope effects on the formation and anaerobic oxidation of methane. *J. Am. Chem. Soc. 135*, 14975−14984.

(17) Schönheit, P., Moll, J., and Thauer, R. K. (1979) Nickel, cobalt, and molybdenum requirement for growth of *Methanobacterium thermoautotrophicum*. *Arch. Microbiol. 123*, 105−107.

(18) Whitman, W. B., and Wolfe, R. S. (1980) Presence of nickel in factor F-430 from *Methanobacterium bryantii*. *Biochem. Biophys. Res. Commun. 92*, 1196−1201.

(19) Diekert, G., Klee, B., and Thauer, R. K. (1980) Nickel, a component of factor-F430 from *Methanobacterium thermoautotrophicum*. *Arch. Microbiol. 124*, 103−106.

(20) Ellefson, W. L., and Wolfe, R. S. (1980) Role of component-C in the methylreductase system of *Methanobacterium*. *J. Biol. Chem. 255*, 8388−8389.

(21) Diekert, G., Gilles, H. H., Jaenchen, R., and Thauer, R. K. (1980) Incorporation of 8 succinate per mol nickel into factors-F-430 by *Methanobacterium thermoautotrophicum*. *Arch. Microbiol. 128*, 256−262.

(22) Diekert, G., Jaenchen, R., and Thauer, R. K. (1980) Biosynthetic evidence for a nickel tetrapyrrole structure of factor F430 from *Methanobacterium thermoautotrophicum*. *FEBS Lett. 119*, 118−120.

(23) Jaenchen, R., Diekert, G., and Thauer, R. K. (1981) Incorporation of methionine-derived methyl-groups into factor-F430 by *Methanobacterium thermoautotrophicum*. *FEBS Lett. 130*, 133−136.

(24) Jaenchen, R., Gilles, H. H., and Thauer, R. K. (1981) Inhibition of factor F-430 synthesis by levulinic acid in *Methanobacterium thermoautotrophicum*. *FEMS Microbiol. Lett. 12*, 167−170.

(25) Farber, G., Keller, W., Kratky, C., Jaun, B., Pfaltz, A., Spinner, C., Kobelt, A., and Eschenmoser, A. (1991) Coenzyme F430 from methanogenic Bacteria - Complete assignment of configuration based on an X-ray-analysis of 12,13-diepi-F430 pentamethyl Ester and on NMR-spectroscopy. *Helv. Chim. Acta 74*, 697−716.

(26) Fässler, A., Kobelt, A., Pfaltz, A., Eschenmoser, A., Bladon, C., Battersby, A. R., and Thauer, R. K. (1985) Factor F430 from methanogenic bacteria - Absolute-configuration. *Helv. Chim. Acta 68*, 2287−2298.

(27) Livingston, D. A., Pfaltz, A., Schreiber, J., Eschnmoser, A., Ankelfuchs, D., Moll, J., Jaenchen, R., and Thauer, R. K. (1984) Factor-F430 from methanogenic bacteria - Structure of the protein-free factor. *Helv. Chim. Acta 67*, 334−351.

(28) Pfaltz, A., Jaun, B., Fassler, A., Eschenmoser, A., Jaenchen, R., Gilles, H. H., Diekert, G., and Thauer, R. K. (1982) Factor-F430 from methanogenic bacteria - Structure of the porphinoid ligand system. *Helv. Chim. Acta 65*, 828−865.

(29) Thauer, R. K. (2015) My lifelong passion for biochemistry and anaerobic microorganisms. *Annu. Rev. Microbiol. 69*, 1−30.

(30) Keltjens, J. T., Whitman, W. B., Caerteling, C. G., Vankooten, A. M., Wolfe, R. S., and Vogels, G. D. (1982) Presence of coenzyme M derivatives in the prosthetic group (Coenzyme-M F430) of methylcoenzyme-M reductase from *Methanobacterium thermoautotrophicum*. *Biochem. Biophys. Res. Commun. 108*, 495−503.

(31) Hüster, R., Gilles, H. H., and Thauer, R. K. (1985) Is coenzyme M bound to factor F430 in methanogenic bacteria - Experiments with *Methanobrevibacter ruminantium*. *Eur. J. Biochem. 148*, 107−111.

(32) Rospert, S., Bocher, R., Albracht, S. P. J., and Thauer, R. K. (1991) Methyl-coenzyme-M reductase preparations with high specific activity from H_2-preincubated cells of *Methanobacterium thermoautotrophicum*. *FEBS Lett. 291*, 371−375.

(33) Goubeaud, M., Schreiner, G., and Thauer, R. K. (1997) Purified methyl-coenzyme-M reductase is activated when the enzyme-bound coenzyme F430 is reduced to the nickel(I) oxidation state by titanium(III) citrate. *Eur. J. Biochem. 243*, 110−114.

(34) Moore, S. J., Sowa, S. T., Schuchardt, C., Deery, E., Lawrence, A. D., Ramos, J. V., Billig, S., Birkemeyer, C., Chivers, P. T., Howard, M. J., Rigby, S. E. J., Layer, G., and Warren, M. J. (2017) Elucidation of the biosynthesis of the methane catalyst coenzyme F-430. *Nature 543*, 78−82.

(35) Zheng, K. Y., Ngo, P. D., Owens, V. L., Yang, X. P., and Mansoorabadi, S. O. (2016) The biosynthetic pathway of coenzyme F430 in methanogenic and methanotrophic archaea. *Science 354*, 339−342.

DOI: 10.1021/acs.biochem.9b00164
Biochemistry 2019, 58, 5198−5220

(36) Scheller, S., Goenrich, M., Boecher, R., Thauer, R. K., and Jaun, B. (2010) The key nickel enzyme of methanogenesis catalyses the anaerobic oxidation of methane. *Nature 465*, 606−608.
(37) Hallam, S. J., Girguis, P. R., Preston, C. M., Richardson, P. M., and DeLong, E. F. (2003) Identification of methyl coenzyme M reductase A (mcrA) genes associated with methane-oxidizing archaea. *Appl. Environ. Microb 69*, 5483−5491.
(38) Krüger, M., Meyerdierks, A., Glockner, F. O., Amann, R., Widdel, F., Kube, M., Reinhardt, R., Kahnt, R., Bocher, R., Thauer, R. K., and Shima, S. (2003) A conspicuous nickel protein in microbial mats that oxidize methane anaerobically. *Nature 426*, 878−881.
(39) Thauer, R. K. (2010) Functionalization of methane in anaerobic microorganisms. *Angew. Chem., Int. Ed. 49*, 6712−6713.
(40) Ragsdale, S. W., Raugei, S., Ginovska, B., and Wongnate, T. (2017) Biochemistry of methyl-coenzyme M reductase. In *Biological Chemistry of Nickel* (Zamble, D., Rowinska-Zyrek, M., and Koslowski, Eds.), Chapter 8, pp 149−169, Royal Society of Chemistry, Cambridge.
(41) Kallistova, A. Y., Merkel, A. Y., Tarnovetskii, I. Y., and Pimenov, N. V. (2017) Methane formation and oxidation by prokaryotes. *Microbiology 86*, 671−691.
(42) Thauer, R. K., Kaster, A. K., Seedorf, H., Buckel, W., and Hedderich, R. (2008) Methanogenic archaea: ecologically relevant differences in energy conservation. *Nat. Rev. Microbiol. 6*, 579−591.
(43) Boetius, A., Ravenschlag, K., Schubert, C. J., Rickert, D., Widdel, F., Gieseke, A., Amann, R., Jorgensen, B. B., Witte, U., and Pfannkuche, O. (2000) A marine microbial consortium apparently mediating anaerobic oxidation of methane. *Nature 407*, 623−626.
(44) Boetius, A., and Wenzhofer, F. (2013) Seafloor oxygen consumption fuelled by methane from cold seeps. *Nat. Geosci. 6*, 725−734.
(45) Ijiri, A., Inagaki, F., Kubo, Y., Adhikari, R. R., Hattori, S., Hoshino, T., Imachi, H., Kawagucci, S., Morono, Y., Ohtomo, Y., Ono, S., Sakai, S., Takai, K., Toki, T., Wang, D. T., Yoshinaga, M. Y., Arnold, G. L., Ashi, J., Case, D. H., Feseker, T., Hinrichs, K. U., Ikegawa, Y., Ikehara, M., Kallmeyer, J., Kumagai, H., Lever, M. A., Morita, S., Nakamura, K. I., Nakamura, Y., Nishizawa, M., Orphan, V. J., Roy, H., Schmidt, F., Tani, A., Tanikawa, W., Terada, T., Tomaru, H., Tsuji, T., Tsunogai, U., Yamaguchi, Y. T., and Yoshida, N. (2018) Deep-biosphere methane production stimulated by geofluids in the Nankai accretionary complex. *Sci. Adv. 4*, eaao4631.
(46) Scheller, S., Ermler, U., and Shima, S. (2017) Catabolic pathways and enzymes involved in anaerobic methane oxidation. In *Anaerobic utilization of hydrocarbons, oils and lipids. Handbook of Hydrocarbons and Lipid microbiology* (Boll, M., Ed.) pp 1−29, Springer International Publishing AG.
(47) Evans, P. N., Boyd, J. A., Leu, A. O., Woodcroft, B. J., Parks, D. H., Hugenholtz, P., and Tyson, G. W. (2019) An evolving view of methane metabolism in the Archaea. *Nat. Rev. Microbiol. 17*, 219.
(48) Semrau, J. D., DiSpirito, A. A., Gu, W. Y., and Yoon, S. (2018) Metals and methanotrophy. *Appl. Environ. Microbiol. 84*, 1−17.
(49) Conrad, R. (2009) The global methane cycle: recent advances in understanding the microbial processes involved. *Environ. Microbiol. Rep. 1*, 285−292.
(50) Yvon-Durocher, G., Allen, A. P., Bastviken, D., Conrad, R., Gudasz, C., St-Pierre, A., Thanh-Duc, N., and del Giorgio, P. A. (2014) Methane fluxes show consistent temperature dependence across microbial to ecosystem scales. *Nature 507*, 488−491.
(51) Joiner, J., Yoshida, Y., Zhang, Y., Duveiller, G., Jung, M., Lyapustin, A., Wang, Y. J., and Tucker, C. J. (2018) Estimation of terrestrial global gross primary production (GPP) with satellite data-driven models and Eddy covariance flux data. *Remote Sens-Basel 10*, 1346−1384.
(52) del Giorgio, P. A., and Duarte, C. M. (2002) Respiration in the open ocean. *Nature 420*, 379−384.
(53) Singh, R., Guzman, M. S., and Bose, A. (2017) Anaerobic oxidation of ethane, propane, and butane by marine microbes: A mini review. *Front. Microbiol. 8*, 1−8.
(54) Laso-Perez, R., Wegener, G., Knittel, K., Widdel, F., Harding, K. J., Krukenberg, V., Meier, D. V., Richter, M., Tegetmeyer, H. E., Riedel, D., Richnow, H. H., Adrian, L., Reemtsma, T., Lechtenfeld, O. J., and Musat, F. (2016) Thermophilic archaea activate butane via alkyl-coenzyme M formation. *Nature 539*, 396−401.
(55) Chen, S., Musat, N., Lechtenfeld, O. J., Paschke, H., Schmidt, M., Said, N., Popp, D., Calabrese, F., Stryhanyuk, H., Jaekel, U., Zhu, Y. G., Joye, S. B., Richnow, H. H., Widdel, F., and Musat, F. (2019) Anaerobic oxidation of ethane by archaea from marine hydrocarbon seep. *Nature*, 1 DOI: 10.1038/s41586-019-1063-0.
(56) Antonovsky, N., Gleizer, S., and Milo, R. (2017) Engineering carbon fixation in *E. coil*: from heterologous RuBisCO expression to the Calvin-Benson-Bassham cycle. *Curr. Opin. Biotechnol. 47*, 83−91.
(57) Takano, Y., Kaneko, M., Kahnt, J., Imachi, H., Shima, S., and Ohkouchi, N. (2013) Detection of coenzyme F430 in deep sea sediments: A key molecule for biological methanogenesis. *Org. Geochem. 58*, 137−140.
(58) Kaneko, M., Takano, Y., Chikaraishi, Y., Ogawa, N. O., Asakawa, S., Watanabe, T., Shima, S., Kruger, M., Matsushita, M., Kimura, H., and Ohkouchi, N. (2014) Quantitative analysis of coenzyme F430 in environmental samples: A new diagnostic tool for methanogenesis and anaerobic methane oxidation. *Anal. Chem. 86*, 3633−3638.
(59) Passaris, I., Van Gaelen, P., Cornelissen, R., Simoens, K., Grauwels, D., Vanhaecke, L., Springael, D., and Smets, I. (2018) Cofactor F430 as a biomarker for methanogenic activity: application to an anaerobic bioreactor system. *Appl. Microbiol. Biotechnol. 102*, 1191−1201.
(60) Shima, S., Krueger, M., Weinert, T., Demmer, U., Kahnt, J., Thauer, R. K., and Ermler, U. (2012) Structure of a methyl-coenzyme M reductase from Black Sea mats that oxidize methane anaerobically. *Nature 481*, 98−101.
(61) Wagner, T., Wegner, C. E., Kahnt, J., Ermler, U., and Shima, S. (2017) Phylogenetic and structural comparisons of the three types of methyl coenzyme M reductase from Methanococcales and Methanobacteriales. *J. Bacteriol. 199*, 1−15.
(62) Lueders, T., Chin, K. J., Conrad, R., and Friedrich, M. (2001) Molecular analyses of methyl-coenzyme M reductase alpha-subunit (mcrA) genes in rice field soil and enrichment cultures reveal the methanogenic phenotype of a novel archaeal lineage. *Environ. Microbiol. 3*, 194−204.
(63) Steinberg, L. M., and Regan, J. M. (2009) mcrA-targeted real-time quantitative PCR method to examine methanogen communities. *Appl. Environ. Microb 75*, 4435−4442.
(64) Losekann, T., Knittel, K., Nadalig, T., Fuchs, B., Niemann, H., Boetius, A., and Amann, R. (2007) Diversity and abundance of aerobic and anaerobic methane oxidizers at the Haakon Mosby mud volcano, Barents Sea. *Appl. Environ. Microb 73*, 3348−3362.
(65) Sakai, S., Imachi, H., Hanada, S., Ohashi, A., Harada, H., and Kamagata, Y. (2008) *Methanocella paludicola* gen. nov., sp nov., a methane-producing archaeon, the first isolate of the lineage 'Rice Cluster I', and proposal of the new archaeal order Methanocellales ord. nov. *Int. J. Syst. Evol. Microbiol. 58*, 929−936.
(66) Borrel, G., Parisot, N., Harris, H. M. B., Peyretaillade, E., Gaci, N., Tottey, W., Bardot, O., Raymann, K., Gribaldo, S., Peyret, P., O'Toole, P. W., and Brugere, J. F. (2014) Comparative genomics highlights the unique biology of Methanomassiliicoccales, a Thermoplasmatales-related seventh order of methanogenic archaea that encodes pyrrolysine. *BMC Genomics 15*, 679.
(67) Lang, K., Schuldes, J., Klingl, A., Poehlein, A., Daniel, R., and Brune, A. (2015) New mode of energy metabolism in the seventh order of methanogens as revealed by comparative genome analysis of "Candidatus *Methanoplasma* termitum". *Appl. Environ. Microbiol. 81*, 1338−1352.
(68) Sorokin, D. Y., Messina, E., Smedile, F., Roman, P., Damste, J. S. S., Ciordia, S., Mena, M. C., Ferrer, M., Golyshin, P. N., Kublanov, I. V., Samarov, N. I., Toshchakov, S. V., La Cono, V., and Yakimov, M. M. (2017) Discovery of anaerobic lithoheterotrophic haloarchaea, ubiquitous in hypersaline habitats. *ISME J. 11*, 1245−1260.

DOI: 10.1021/acs.biochem.9b00164
Biochemistry 2019, 58, 5198−5220

(69) Boyd, J. A., Jungbluth, S. P., Leu, A. O., Evans, P. N., Woodcroft, B. J., Chadwick, G. L., Orphan, V. J., Amend, J. P., Rappe, M. S., and Tyson, G. W. (2019) Divergent methyl-coenzyme M reductase genes in a deep-subseafloor Archaeoglobi. *ISME J.*, 1.
(70) Evans, P. N., Parks, D. H., Chadwick, G. L., Robbins, S. J., Orphan, V. J., Golding, S. D., and Tyson, G. W. (2015) Methane metabolism in the archaeal phylum Bathyarchaeota revealed by genome-centric metagenomics. *Science 350*, 434−438.
(71) Vanwonterghem, I., Evans, P. N., Parks, D. H., Jensen, P. D., Woodcroft, B. J., Hugenholtz, P., and Tyson, G. W. (2016) Methylotrophic methanogenesis discovered in the archaeal phylum Verstraetearchaeota. *Nat. Microbiol 1*, 1−9.
(72) McKay, L. J., Hatzenpichler, R., Inskeep, W. P., and Fields, M. W. (2017) Occurrence and expression of novel methyl-coenzyme M reductase gene (mcrA) variants in hot spring sediments. *Sci. Rep. 7*, 1−12.
(73) Fuchs, G., Stupperich, E., and Thauer, R. K. (1978) Function of fumarate reductase in methanogenic bacteria (*Methanobacterium*). *Arch. Microbiol. 119*, 215−218.
(74) Schönheit, P., Moll, J., and Thauer, R. K. (1980) Growth-parameters (Ks, Mu-Max, Ys) of *Methanobacterium thermoautotrophicum*. *Arch. Microbiol. 127*, 59−65.
(75) Thauer, R. K., Kaster, A. K., Goenrich, M., Schick, M., Hiromoto, T., and Shima, S. (2010) Hydrogenases from methanogenic archaea, nickel, a novel cofactor, and H_2 storage. *Annu. Rev. Biochem. 79*, 507−536.
(76) Buckel, W., and Thauer, R. K. (2013) Energy conservation via electron bifurcating ferredoxin reduction and proton/Na+ translocating ferredoxin oxidation. *Biochim. Biophys. Acta, Bioenerg. 1827*, 94−113.
(77) Buckel, W., and Thauer, R. K. (2018) Flavin-based electron bifurcation, a new mechanism of biological energy coupling. *Chem. Rev. 118*, 3862−3886.
(78) Buckel, W., and Thauer, R. K. (2018) Flavin-based electron bifurcation, ferredoxin, flavodoxin, and anaerobic respiration with protons (Ech) or NAD^+ (Rnf) as electron acceptors: A historical review. *Front. Microbiol. 9*, 1−24.
(79) Albracht, S. P. J., Ankel-Fuchs, D., Bocher, R., Ellermann, J., Moll, J., Vanderzwaan, J. W., and Thauer, R. K. (1988) 5 New electron-paramagnetic-res signals assigned to nickel in methyl-coenzyme M-reductase from *Methanobacterium-thermoautotrophicum*, Strain Marburg. *Biochim. Biophys. Acta, Protein Struct. Mol. Enzymol. 955*, 86−102.
(80) Tietze, M., Beuchle, A., Lamla, I., Orth, N., Dehler, M., Greiner, G., and Beifuss, U. (2003) Redox potentials of methanophenazine and CoB-S-S-CoM, factors involved in electron transport in methanogenic archaea. *ChemBioChem 4*, 333−335.
(81) Duin, E. C., Signor, L., Piskorski, R., Mahlert, F., Clay, M. D., Goenrich, M., Thauer, R. K., Jaun, B., and Johnson, M. K. (2004) Spectroscopic investigation of the nickel-containing porphinoid cofactor F-430. Comparison of the free cofactor in the + 1, + 2 and + 3 oxidation states with the cofactor bound to methyl-coenzyme M reductase in the silent, red and ox forms. *JBIC, J. Biol. Inorg. Chem. 9*, 563−576.
(82) Mahlert, F., Bauer, C., Jaun, B., Thauer, R. K., and Duin, E. C. (2002) The nickel enzyme methyl-coenzyme M reductase from methanogenic archaea: In vitro induction of the nickel-based MCR-ox EPR signals from MCR-red2. *JBIC, J. Biol. Inorg. Chem. 7*, 500−513.
(83) Mahlert, F., Grabarse, W., Kahnt, J., Thauer, R. K., and Duin, E. C. (2002) The nickel enzyme methyl-coenzyme M reductase from methanogenic archaea: in vitro interconversions among the EPR detectable MCR-red1 and MCR-red2 states. *JBIC, J. Biol. Inorg. Chem. 7*, 101−112.
(84) Jaun, B., and Pfaltz, A. (1986) Coenzyme-F430 from methanogenic bacteria - Reversible one-electron reduction of F430 pentamethyl ester to the Nickel(I) form. *J. Chem. Soc., Chem. Commun.*, 1327−1329.
(85) Holliger, C., Pierik, A. J., Reijerse, E. J., and Hagen, W. R. (1993) A spectroelectrochemical study of factor F430 nickel(Ii/I) from methanogenic bacteria in aqueous-solution. *J. Am. Chem. Soc. 115*, 5651−5656.
(86) Becker, D. F., and Ragsdale, S. W. (1998) Activation of methyl-S-CoM reductase to high specific activity after treatment of whole cells with sodium sulfide. *Biochemistry 37*, 2639−2647.
(87) Singh, K., Horng, Y. C., and Ragsdale, S. W. (2003) Rapid ligand exchange in the MCRred1 form of methyl-coenzyme m reductase. *J. Am. Chem. Soc. 125*, 2436−2443.
(88) Telser, J., Horng, Y. C., Becker, D. F., Hoffman, B. M., and Ragsdale, S. W. (2000) On the assignment of nickel oxidation states of the Ox1, Ox2 forms of methyl-coenzyme M reductase. *J. Am. Chem. Soc. 122*, 182−183.
(89) Jaun, B. (1990) Coenzyme-F430 from methanogenic bacteria - Oxidation of F430 pentamethyl ester to the Ni(Iii) form. *Helv. Chim. Acta 73*, 2209−2217.
(90) Harmer, J., Finazzo, C., Piskorski, R., Bauer, C., Jaun, B., Duin, E. C., Goenrich, M., Thauer, R. K., Van Doorslaer, S., and Schweiger, A. (2005) Spin density and coenzyme M coordination geometry of the ox1 form of methyl-coenzyme M reductase: A pulse EPR study. *J. Am. Chem. Soc. 127*, 17744−17755.
(91) Dey, M., Kunz, R. C., Lyons, D. M., and Ragsdale, S. W. (2007) Characterization of alkyl-nickel adducts generated by reaction of methyl-coenzyme M reductase with brominated acids. *Biochemistry 46*, 11969−11978.
(92) Dey, M., Telser, J., Kunz, R. C., Lees, N. S., Ragsdale, S. W., and Hoffman, B. M. (2007) Biochemical and spectroscopic studies of the electronic structure and reactivity of a methyl-Ni species formed on methyl-coenzyme M reductase. *J. Am. Chem. Soc. 129*, 11030−11032.
(93) Telser, J., Davydov, R., Horng, Y. C., Ragsdale, S. W., and Hoffman, B. M. (2001) Cryoreduction of methyl-coenzyme M reductase: EPR characterization of forms, MCRox1 and MCRred1. *J. Am. Chem. Soc. 123*, 5853−5860.
(94) Tang, Q., Carrington, P. E., Horng, Y. C., Maroney, M. J., Ragsdale, S. W., and Bocian, D. F. (2002) X-ray absorption and resonance Raman studies of methyl-coenzyme M reductase indicating that ligand exchange and macrocycle reduction accompany reductive activation. *J. Am. Chem. Soc. 124*, 13242−13256.
(95) Piskorski, R., and Jaun, B. (2003) Direct determination of the number of electrons needed to reduce coenzyme F430 pentamethyl ester to the Ni(I) species exhibiting the electron paramagnetic resonance and ultraviolet-visible spectra characteristic for the MCRred1 state of methyl-coenzyme M reductase. *J. Am. Chem. Soc. 125*, 13120−13125.
(96) Craft, J. L., Horng, Y. C., Ragsdale, S. W., and Brunold, T. C. (2004) Spectroscopic and computational characterization of the nickel-containing F-430 cofactor of methyl-coenzyme M reductase. *JBIC, J. Biol. Inorg. Chem. 9*, 77−89.
(97) Craft, J. L., Horng, Y. C., Ragsdale, S. W., and Brunold, T. C. (2004) Nickel oxidation states of F-430 cofactor in methyl-coenzyme M reductase. *J. Am. Chem. Soc. 126*, 4068−4069.
(98) Dey, M., Kunz, R. C., Van Heuvelen, K. M., Craft, J. L., Horng, Y. C., Tang, Q., Bocian, D. F., George, S. J., Brunold, T. C., and Ragsdale, S. W. (2006) Spectroscopic and computational studies of reduction of the metal versus the tetrapyrrole ring of coenzyme F-430 from methyl-coenzyme M reductase. *Biochemistry 45*, 11915−11933.
(99) Mayer, F., Rohde, M., Salzmann, M., Jussofie, A., and Gottschalk, G. (1988) The methanoreductosome - a high-molecular-weight enzyme complex in the methanogenic bacterium Strain Go1 that contains components of the methylreductase system. *J. Bacteriol. 170*, 1438−1444.
(100) Ossmer, R., Mund, T., Hartzell, P. L., Konheiser, U., Kohring, G. W., Klein, A., Wolfe, R. S., Gottschalk, G., and Mayer, F. (1986) Immunocytochemical localization of component-C of the methyl-reductase system in *Methanococcus voltae* and *Methanobacterium thermoautotrophicum*. *Proc. Natl. Acad. Sci. U. S. A. 83*, 5789−5792.
(101) Aldrich, H. C., Beimborn, D. B., Bokranz, M., and Schönheit, P. (1987) Immunocytochemical localization of methyl-coenzyme-M reductase in *Methanobacterium-thermoautotrophicum*. *Arch. Microbiol. 147*, 190−194.

DOI: 10.1021/acs.biochem.9b00164
Biochemistry 2019, 58, 5198−5220

(102) Sauer, F. D., Erfle, J. D., and Mahadevan, S. (1980) Methane production by the membranous fraction of *Methanobacterium thermoautotrophicum*. *Biochem. J. 190*, 177−182.
(103) Wrede, C., Walbaum, U., Ducki, A., Heieren, I., and Hoppert, M. (2013) Localization of methyl-coenzyme M reductase as metabolic marker for diverse methanogenic archaea. *Archaea 2013*, 1−7.
(104) Rospert, S., Linder, D., Ellermann, J., and Thauer, R. K. (1990) 2 genetically distinct methyl-coenzyme M reductases in *Methanobacterium thermoautotrophicum* Strain Marburg and Delta-H. *Eur. J. Biochem. 194*, 871−877.
(105) Bonacker, L. G., Baudner, S., and Thauer, R. K. (1992) Differential expression of the 2 methyl-coenzyme M reductases in Methanobacterium thermoautotrophicum as determined immunochemically via isoenzyme-specific antisera. *Eur. J. Biochem. 206*, 87−92.
(106) Pihl, T. D., Sharma, S., and Reeve, J. N. (1994) Growth phase-dependent transcription of the genes that encode the 2 methyl coenzyme-M reductase isoenzymes and N-5-methyltetrahydromethanopterin-coenzyme-M methyltransferase in *Methanobacterium thermoautotrophicum* Delta-H. *J. Bacteriol. 176*, 6384−6391.
(107) Bonacker, L. G., Baudner, S., Morschel, E., Bocher, R., and Thauer, R. K. (1993) Properties of the 2 isoenzymes of methyl-coenzyme-M reductase in *Methanobacterium thermoautotrophicum*. *Eur. J. Biochem. 217*, 587−595.
(108) Cram, D. S., Sherf, B. A., Libby, R. T., Mattaliano, R. J., Ramachandran, K. L., and Reeve, J. N. (1987) Structure and expression of the genes, *McrBDCGA*, which encode the subunits of component-C of methyl coenzyme-M reductase in *Methanococcus vannielii*. *Proc. Natl. Acad. Sci. U. S. A. 84*, 3992−3996.
(109) Bokranz, M., and Klein, A. (1987) Nucleotide-sequence of the methyl coenzyme-M reductase gene-cluster from *Methanosarcina barkeri*. *Nucleic Acids Res. 15*, 4350−4351.
(110) Allmansberger, R., Bollschweiler, C., Konheiser, U., Müller, B., Muth, E., Pasti, G., and Klein, A. (1986) Arrangement and expression of methyl coenzyme M reductase genes in *Methanococcus voltae*. *Syst. Appl. Microbiol. 7*, 13−17.
(111) Ellermann, J., Rospert, S., Thauer, R. K., Bokranz, M., Klein, A., Voges, M., and Berkessel, A. (1989) Methyl-coenzyme-M reductase from *Methanobacterium thermoautotrophicum* (Strain Marburg) - Purity, activity and novel inhibitors. *Eur. J. Biochem. 184*, 63−68.
(112) Lyu, Z., Chou, C. W., Shi, H., Wang, L. L., Ghebreab, R., Phillips, D., Yan, Y. J., Duin, E. C., and Whitman, W. B. (2018) Assembly of methyl coenzyme M reductase in the methanogenic archaeon *Methanococcus maripaludis*. *J. Bacteriol. 200*, 1−12.
(113) Prakash, D., Wu, Y., Suh, S., and Duin, E. C. (2014) Elucidating the process of activation of methyl-coenzyme M reductase. *J. Bacteriol. 196*, 2491−2498.
(114) Jablonski, P. E., and Ferry, J. G. (1991) Purification and properties of methyl coenzyme-M methylreductase from acetate-grown *Methanosarcina thermophila*. *J. Bacteriol. 173*, 2481−2487.
(115) Sauer, F. D. (1991) Inhibition of methylcoenzyme-M methylreductase by a uridine 5′-diphospho-N-acetylglucosamine derivative. *Biochem. Biophys. Res. Commun. 174*, 619−624.
(116) Sauer, F. D., Blackwell, B. A., Kramer, J. K. G., and Marsden, B. J. (1990) Isolation and characterization of the carbohydrate moiety bound to N-7-mercaptoheptanoyl-O-threonine phosphate. *FEMS Microbiol. Lett. 87*, 333−338.
(117) Ermler, U., Grabarse, W., Shima, S., Goubeaud, M., and Thauer, R. K. (1997) Crystal structure of methyl coenzyme M reductase: The key enzyme of biological methane formation. *Science 278*, 1457−1462.
(118) Grabarse, W., Mahlert, F., Duin, E. C., Goubeaud, M., Shima, S., Thauer, R. K., Lamzin, V., and Ermler, U. (2001) On the mechanism of biological methane formation: Structural evidence for conformational changes in methyl-coenzyme M reductase upon substrate binding. *J. Mol. Biol. 309*, 315−330.
(119) Cedervall, P. E., Dey, M., Pearson, A. R., Ragsdale, S. W., and Wilmot, C. M. (2010) Structural insight into methyl-coenzyme M reductase chemistry using coenzyme B analogues. *Biochemistry 49*, 7683−7693.
(120) Cedervall, P. E., Dey, M., Li, X. H., Sarangi, R., Hedman, B., Ragsdale, S. W., and Wilmot, C. M. (2011) Structural analysis of a Ni-methyl species in methyl-coenzyme M reductase from *Methanothermobacter marburgensis*. *J. Am. Chem. Soc. 133*, 5626−5628.
(121) Grabarse, W. G., Mahlert, F., Shima, S., Thauer, R. K., and Ermler, U. (2000) Comparison of three methyl-coenzyme M reductases from phylogenetically distant organisms: Unusual amino acid modification, conservation and adaptation. *J. Mol. Biol. 303*, 329−344.
(122) Mayr, S., Latkoczy, C., Kruger, M., Gunther, D., Shima, S., Thauer, R. K., Widdel, F., and Jaun, B. (2008) Structure of an F430 variant from archaea associated with anaerobic oxidation of methane. *J. Am. Chem. Soc. 130*, 10758−10767.
(123) Soo, V. W. C., McAnulty, M. J., Tripathi, A., Zhu, F. Y., Zhang, L. M., Hatzakis, E., Smith, P. B., Agrawal, S., Nazem-Bokaee, H., Gopalakrishnan, S., Salis, H. M., Ferry, J. G., Maranas, C. D., Patterson, A. D., and Wood, T. K. (2016) Reversing methanogenesis to capture methane for liquid biofuel precursors. *Microb. Cell Fact. 15*, 1−14.
(124) Allen, K. D., Wegener, G., and White, R. H. (2014) Discovery of multiple modified F-430 coenzymes in methanogens and anaerobic methanotrophic archaea suggests possible new roles for F-430 in nature. *Appl. Environ. Microbiol. 80*, 6403−6412.
(125) Selmer, T., Kahnt, J., Goubeaud, M., Shima, S., Grabarse, W., Ermler, U., and Thauer, R. K. (2000) The biosynthesis of methylated amino acids in the active site region of methyl-coenzyme M reductase. *J. Biol. Chem. 275*, 3755−3760.
(126) Kahnt, J., Buchenau, B., Mahlert, F., Kruger, M., Shima, S., and Thauer, R. K. (2007) Post-translational modifications in the active site region of methyl-coenzyme M reductase from methanogenic and methanotrophic archaea. *FEBS J. 274*, 4913−4921.
(127) Nayak, D. D., Mahanta, N., Mitchell, D. A., and Metcalf, W. W. (2017) Post-translational thioamidation of methyl-coenzyme M reductase, a key enzyme in methanogenic and methanotrophic Archaea. *eLife 6*, 1−18.
(128) Mahanta, N., Liu, A. D., Dong, S. H., Nair, S. K., and Mitchell, D. A. (2018) Enzymatic reconstitution of ribosomal peptide backbone thioamidation. *Proc. Natl. Acad. Sci. U. S. A. 115*, 3030−3035.
(129) Nayak, D. D., and Metcalf, W. W. (2018) Genetic techniques for studies of methyl-coenzyme M reductase from *Methanosarcina acetivorans* C2A. *Methods Enzymol. 613*, 325−347.
(130) Deobald, D., Adrian, L., Schone, C., Rother, M., and Layer, G. (2018) Identification of a unique Radical SAM methyltransferase required for the sp(3)-C-methylation of an arginine residue of methyl-coenzyme M reductase. *Sci. Rep. 8*, 1−12.
(131) Thauer, R. K., Jungermann, K., and Decker, K. (1977) Energy-conservation in chemotropic anaerobic bacteria. *Bacteriol Rev. 41*, 100−180.
(132) Stroup, D., and Reeve, J. N. (1993) Association of the McrD gene-product with methyl coenzyme M-reductase in *Methanococcus vannielii*. *Biochim. Biophys. Acta, Protein Struct. Mol. Enzymol. 1203*, 175−183.
(133) Goenrich, M., Mahlert, F., Duin, E. C., Bauer, C., Jaun, B., and Thauer, R. K. (2004) Probing the reactivity of Ni in the active site of methyl-coenzyme M reductase with substrate analogues. *JBIC, J. Biol. Inorg. Chem. 9*, 691−705.
(134) Ellermann, J., Kobelt, A., Pfaltz, A., and Thauer, R. K. (1987) On the role of N-7-mercaptoheptanoyl-O-phospho-L-threonine (Component B) in the enzymatic reduction of methyl-coenzyme-M to methane. *FEBS Lett. 220*, 358−362.
(135) Goenrich, M., Duin, E. C., Mahlert, F., and Thauer, R. K. (2005) Temperature dependence of methyl-coenzyme M reductase activity and of the formation of the methyl-coenzyme M reductase red2 state induced by coenzyme B. *JBIC, J. Biol. Inorg. Chem. 10*, 333−342.

DOI: 10.1021/acs.biochem.9b00164
Biochemistry 2019, 58, 5198−5220

(136) Wongnate, T., Sliwa, D., Ginovska, B., Smith, D., Wolf, M. W., Lehnert, N., Raugei, S., and Ragsdale, S. W. (2016) The radical mechanism of biological methane synthesis by methyl-coenzyme M reductase. *Science 352*, 953−958.
(137) Ahn, Y., Krzycki, J., and Floss, H. G. (1991) Steric course of reduction of ethyl-coenzyme M to ethane catalyzed by methyl-coenzyme M reductase from *Methanosarcina barkeri*. *J. Am. Chem. Soc. 113*, 4700−4701.
(138) Scheller, S., Goenrich, M., Thauer, R. K., and Jaun, B. (2013) Methyl-coenzyme M reductase from methanogenic Archaea: Isotope effects on label exchange and ethane formation with the homologous substrate ethyl-coenzyme M. *J. Am. Chem. Soc. 135*, 14985−14995.
(139) Gunsalus, R. P., Romesser, J. A., and Wolfe, R. S. (1978) Preparation of coenzyme-M analogs and their activity in methyl coenzyme-M reductase system of *Methanobacterium thermoautotrophicum*. *Biochemistry 17*, 2374−2377.
(140) Balch, W. E., and Wolfe, R. S. (1979) Specificity and biological distribution of coenzyme M (2-mercaptoethanesulfonic acid). *J. Bacteriol. 137*, 256−263.
(141) Wackett, L. P., Honek, J. F., Begley, T. P., Wallace, V., Ormejohnson, W. H., and Walsh, C. T. (1987) Substrate-analogs as mechanistic probes of methyl-S-coenzyme-M reductase. *Biochemistry 26*, 6012−6018.
(142) Golicnik, M. (2018) Closed form solution of the reduced Haldane equation for enzyme kinetics with strong substrate inhibition. *Match-Commun. Math Co 79*, 607−618.
(143) Sauer, K., and Thauer, R. K. (1997) Methanol-coenzyme M methyltransferase from *Methanosarcina barkeri* - Zinc dependence and thermodynamics of the methanol:cob(I)alamin methyltransferase reaction. *Eur. J. Biochem. 249*, 280−285.
(144) Thauer, R. K. (1998) Biochemistry of methanogenesis: a tribute to Marjory Stephenson. *Microbiology 144*, 2377−2406.
(145) Holliger, C., Kengen, S. W. M., Schraa, G., Stams, A. J. M., and Zehnder, A. J. B. (1992) Methyl-coenzyme-M reductase of *Methanobacterium thermoautotrophicum* Delta-H catalyzes the reductive dechlorination of 1,2-dichloroethane to ethylene and chloroethane. *J. Bacteriol. 174*, 4435−4443.
(146) Li, X. H., Telser, J., Kunz, R. C., Hoffman, B. M., Gerfen, G., and Ragsdale, S. W. (2010) Observation of organometallic and radical intermediates Formed during the reaction of methyl-coenzyme M reductase with bromoethanesulfonate. *Biochemistry 49*, 6866−6876.
(147) Hinderberger, D., Piskorski, R. R., Goenrich, M., Thauer, R. K., Schweiger, A., Harmer, J., and Jaun, B. (2006) A nickel-alkyl bond in an inactivated state of the enzyme catalyzing methane formation. *Angew. Chem., Int. Ed. 45*, 3602−3607.
(148) Kunz, R. C., Horng, Y. C., and Ragsdale, S. W. (2006) Spectroscopic and kinetic studies of the reaction of bromopropanesulfonate with methyl-coenzyme M reductase. *J. Biol. Chem. 281*, 34663−34676.
(149) Yu, Z. T., and Smith, G. B. (2000) Inhibition of methanogenesis by C-1- and C-2-polychlorinated aliphatic hydrocarbons. *Environ. Toxicol. Chem. 19*, 2212−2217.
(150) Duin, E. C., Wagner, T., Shima, S., Prakash, D., Cronin, B., Yanez-Ruiz, D. R., Duval, S., Rumbeli, R., Stemmler, R. T., Thauer, R. K., and Kindermann, M. (2016) Mode of action uncovered for the specific reduction of methane emissions from ruminants by the small molecule 3-nitrooxypropanol. *Proc. Natl. Acad. Sci. U. S. A. 113*, 6172−6177.
(151) Hristov, A. N., Oh, J., Giallongo, F., Frederick, T. W., Harper, M. T., Weeks, H. L., Branco, A. F., Moate, P. J., Deighton, M. H., Williams, S. R. O., Kindermann, M., and Duval, S. (2015) An inhibitor persistently decreased enteric methane emission from dairy cows with no negative effect on milk production. *Proc. Natl. Acad. Sci. U. S. A. 112*, 10663−10668.
(152) Zhang, Z. W., Cao, Z. J., Wang, Y. L., Wang, Y. J., Yang, H. J., and Li, S. L. (2018) Nitrocompounds as potential methanogenic inhibitors in ruminant animals: A review. *Anim. Feed Sci. Technol. 236*, 107−114.
(153) Schink, B. (1985) Inhibition of methanogenesis by ethylene and other unsaturated hydrocarbons. *FEMS Microbiol. Lett. 31*, 63−68.
(154) Lan, X. W., Wang, N. X., and Xing, Y. L. (2017) Recent advances in radical difunctionalization of simple alkenes. *Eur. J. Org. Chem. 2017*, 5821−5851.
(155) Jaun, B., and Pfaltz, A. (1988) Coenzyme F430 from methanogenic bacteria - Methane formation by reductive carbon sulfur bond-cleavage of methyl sulfonium ions catalyzed by F430 pentamethyl Ester. *J. Chem. Soc., Chem. Commun.*, 293−294.
(156) Lin, S. K., and Jaun, B. (1991) Coenzyme F430 from methanogenic bacteria - Detection of a paramagnetic methylnickel(Ii) derivative of the pentamethyl ester by H_2-NMR spectroscopy. *Helv. Chim. Acta 74*, 1725−1738.
(157) Krone, U. E., Laufer, K., Thauer, R. K., and Hogenkamp, H. P. C. (1989) Coenzyme-F430 as a possible catalyst for the reductive dehalogenation of chlorinated-C_1 hydrocarbons in methanogenic bacteria. *Biochemistry 28*, 10061−10065.
(158) Krone, U. E., Thauer, R. K., and Hogenkamp, H. P. C. (1989) Reductive dehalogenation of chlorinated C_1-hydrocarbons mediated by corrinoids. *Biochemistry 28*, 4908−4914.
(159) Rudiger, H., and Jaenicke, L. (1969) Methionine synthesis - Demonstration of reversibility of reaction. *FEBS Lett. 4*, 316−318.
(160) Thauer, R. K. (2017) Lothar Jaenicke and C-1-metabolism: his first 25 years of research. *Z. Naturforsch., C: J. Biosci. 72*, 237−243.
(161) Yang, N., Reiher, M., Wang, M., Harmer, J., and Duin, E. C. (2007) Formation of a nickel-methyl species in methyl-coenzyme M reductase, an enzyme catalyzing methane formation. *J. Am. Chem. Soc. 129*, 11028−11029.
(162) Sarangi, R., Dey, M., and Ragsdale, S. W. (2009) Geometric and electronic structures of the Ni-I and methyl-Ni-III intermediates of methyl-coenzyme M reductase. *Biochemistry 48*, 3146−3156.
(163) Kunz, R. C., Dey, M., and Ragsdale, S. W. (2008) Characterization of the thioether product formed from the thiolytic cleavage of the alkyl-nickel bond in methyl-coenzyme M reductase. *Biochemistry 47*, 2661−2667.
(164) Dey, M., Li, X. H., Zhou, Y. Z., and Ragsdale, S. W. (2010) Evidence for organometallic intermediates in bacterial methane formation involving the nickel coenzyme F-430. *Metal Ions Life Sci. 7*, 71−110.
(165) Pelmenschikov, V., Blomberg, M. R. A., Siegbahn, P. E. M., and Crabtree, R. H. (2002) A mechanism from quantum chemical studies for methane formation in methanogenesis. *J. Am. Chem. Soc. 124*, 4039−4049.
(166) Pelmenschikov, V., and Siegbahn, P. E. M. (2003) Catalysis by methyl-coenzyme M reductase: a theoretical study for heterodisulfide product formation. *JBIC, J. Biol. Inorg. Chem. 8*, 653−662.
(167) Chen, S. L., Blomberg, M. R. A., and Siegbahn, P. E. M. (2012) How is methane formed and oxidized reversibly when catalyzed by Ni-containing methyl-coenzyme M reductase? *Chem. - Eur. J. 18*, 6309−6315.
(168) Chen, S. L., Blomberg, M. R. A., and Siegbahn, P. E. M. (2014) An investigation of possible competing mechanisms for Ni-containing methyl-coenzyme M reductase. *Phys. Chem. Chem. Phys. 16*, 14029−14035.
(169) Chen, S. L., Pelmenschikov, V., Blomberg, M. R. A., and Siegbahn, P. E. M. (2009) Is there a Ni-methyl intermediate in the mechanism of methyl-coenzyme M reductase? *J. Am. Chem. Soc. 131*, 9912−9913.
(170) Harmer, J., Finazzo, C., Piskorski, R., Ebner, S., Duin, E. C., Goenrich, M., Thauer, R. K., Reiher, M., Schweiger, A., Hinderberger, D., and Jaun, B. (2008) A nickel hydride complex in the active site of methyl-coenzyme M reductase: Implications for the catalytic cycle. *J. Am. Chem. Soc. 130*, 10907−10920.
(171) Scheller, S., Goenrich, M., Mayr, S., Thauer, R. K., and Jaun, B. (2010) Intermediates in the catalytic cycle of methyl coenzyme M reductase: Isotope exchange is consistent with formation of a sigma-alkane-nickel complex. *Angew. Chem., Int. Ed. 49*, 8112−8115.

DOI: 10.1021/acs.biochem.9b00164
Biochemistry 2019, 58, 5198−5220

(172) Duin, E. C., and Mckee, M. L. (2008) A new mechanism for methane production from methyl-coenzyme M reductase as derived from density functional calculations. *J. Phys. Chem. B 112*, 2466−2482.
(173) Duin, E. C., Cosper, N. J., Mahlert, F., Thauer, R. K., and Scott, R. A. (2003) Coordination and geometry of the nickel atom in active methyl-coenzyme M reductase from *Methanothermobacter marburgensis* as detected by X-ray absorption spectroscopy. *JBIC, J. Biol. Inorg. Chem. 8*, 141−148.
(174) Wongnate, T., and Ragsdale, S. W. (2015) The reaction mechanism of methyl-coenzyme M reductase How an enzyme enforces strict binding order. *J. Biol. Chem. 290*, 9322−9334.
(175) Hinderberger, D., Ebner, S., Mayr, S., Jaun, B., Reiher, M., Goenrich, M., Thauer, R. K., and Harmer, J. (2008) Coordination and binding geometry of methyl-coenzyme M in the red1m state of methyl-coenzyme M reductase. *JBIC, J. Biol. Inorg. Chem. 13*, 1275−1289.
(176) Kern, D. I., Goenrich, M., Jaun, B., Thauer, R. K., Harmer, J., and Hinderberger, D. (2007) Two sub-states of the red2 state of methyl-coenzyme M reductase revealed by high-field EPR spectroscopy. *JBIC, J. Biol. Inorg. Chem. 12*, 1097−1105.
(177) Finazzo, C., Harmer, J., Bauer, C., Jaun, B., Duin, E. C., Mahlert, F., Goenrich, M., Thauer, R. K., Van Doorslaer, S., and Schweiger, A. (2003) Coenzyme B induced coordination of coenzyme M via its thiol group to Ni(I) of F-430 in active methyl-coenzyme M reductase. *J. Am. Chem. Soc. 125*, 4988−4989.
(178) Finazzo, C., Harmer, J., Jaun, B., Duin, E. C., Mahlert, F., Thauer, R. K., Van Doorslaer, S., and Schweiger, A. (2003) Characterization of the MCRred2 form of methyl-coenzyme M reductase: a pulse EPR and ENDOR study. *JBIC, J. Biol. Inorg. Chem. 8*, 586−593.
(179) Ebner, S., Jaun, B., Goenrich, M., Thauer, R. K., and Harmer, J. (2010) Binding of coenzyme B induces a major conformational change in the active site of methyl-coenzyme M reductase. *J. Am. Chem. Soc. 132*, 567−575.
(180) Horng, Y. C., Becker, D. F., and Ragsdale, S. W. (2001) Mechanistic studies of methane biogenesis by methyl-coenzyme M reductase: Evidence that coenzyme B participates in cleaving the C-S bond of methyl-coenzyme M. *Biochemistry 40*, 12875−12885.
(181) Asmus, K. D. (1990) Sulfur-centered free-radicals. *Methods Enzymol. 186*, 168−180.
(182) Roos, G., De Proft, F., and Geerlings, P. (2013) Electron capture by the thiyl radical and disulfide bond: Ligand effects on the reduction potential. *Chem. - Eur. J. 19*, 5050−5060.
(183) Park, C. M., Weerasinghe, L., Day, J. J., Fukuto, J. M., and Xian, M. (2015) Persulfides: current knowledge and challenges in chemistry and chemical biology. *Mol. BioSyst. 11*, 1775−1785.
(184) Rabus, R., Boll, M., Heider, J., Meckenstock, R. U., Buckel, W., Einsle, O., Ermler, U., Golding, B. T., Gunsalus, R. P., Kroneck, P. M. H., Kruger, M., Lueders, T., Martins, B. M., Musat, F., Richnow, H. H., Schink, B., Seifert, J., Szaleniec, M., Treude, T., Ullmann, G. M., Vogt, C., von Bergen, M., and Wilkes, H. (2016) Anaerobic microbial degradation of hydrocarbons: From enzymatic reactions to the environment. *J. Mol. Microb Biotech 26*, 5−28.
(185) Sattler, A. (2018) Hydrogen/Deuterium (H/D) exchange catalysis in alkanes. *ACS Catal. 8*, 2296−2312.
(186) Venkatasubban, K. S., and Schowen, R. L. (1984) The proton inventory technique. *Crc Cr Rev. Bioch Mol. 17*, 1−44.
(187) Mayr, S. (2009) *Struktur einer neuartigen Variante von Cofaktor F430*. Doctoral Thesis Eth Nr. 18459, ETH Zürich, pp 1−278.
(188) Scheller, S. (2011) *Methyl-coenzyme M reductase: Mechanistic studies with ^{2}H and ^{13}C label*. Doctoral Thesis Eth Nr. 19620, ETH Zürich, pp 1−237.
(189) Papish, E. T., Rix, F. C., Spetseris, N., Norton, J. R., and Williams, R. D. (2000) Protonation of CpW(CO)(2)(PMe3)H: Is the metal or the hydride the kinetic site? *J. Am. Chem. Soc. 122*, 12235−12242.
(190) Peruzzini, M., and Poli, R. (2002) *Recent advances in hydride chemistry*, 1st ed., p 55, Elsevier Science.
(191) Wang, D. T., Gruen, D. S., Lollar, B. S., Hinrichs, K. U., Stewart, L. C., Holden, J. F., Hristov, A. N., Pohlman, J. W., Morrill, P. L., Konneke, M., Delwiche, K. B., Reeves, E. P., Sutcliffe, C. N., Ritter, D. J., Seewald, J. S., McIntosh, J. C., Hemond, H. F., Kubo, M. D., Cardace, D., Hoehler, T. M., and Ono, S. (2015) Nonequilibrium clumped isotope signals in microbial methane. *Science 348*, 428−431.
(192) Young, E. D., Kohl, I. E., Lollar, B. S., Etiope, G., Rumble, D., Li, S., Haghnegahdar, M. A., Schauble, E. A., McCain, K. A., Foustoukos, D. I., Sutclife, C., Warr, O., Ballentine, C. J., Onstott, T. C., Hosgormez, H., Neubeck, A., Marques, J. M., Perez-Rodriguez, I., Rowe, A. R., LaRowe, D. E., Magnabosco, C., Yeung, L. Y., Ash, J. L., and Bryndzia, L. T. (2017) The relative abundances of resolved $^{12}CH_2D_2$) and $^{13}CH_3D$ and mechanisms controlling isotopic bond ordering in abiotic and biotic methane gases. *Geochim. Cosmochim. Acta 203*, 235−264.
(193) Gruen, D. S., Wang, D. T., Konneke, M., Topcuoglu, B. D., Stewart, L. C., Goldhammer, T., Holden, J. F., Hinrichs, K. U., and Ono, S. (2018) Experimental investigation on the controls of clumped isotopologue and hydrogen isotope ratios in microbial methane. *Geochim. Cosmochim. Acta 237*, 339−356.
(194) Nagle, D. P., and Wolfe, R. S. (1983) Component-a of the methyl coenzyme-M methylreductase system of *Methanobacterium* - Resolution into 4 components. *Proc. Natl. Acad. Sci. U. S. A. 80*, 2151−2155.
(195) Rouviere, P. E., Escalantesemerena, J. C., and Wolfe, R. S. (1985) Component-A2 of the methylcoenzyme-M methylreductase system from *Methanobacterium thermoautotrophicum*. *J. Bacteriol. 162*, 61−66.
(196) Rouviere, P. E., and Wolfe, R. S. (1987) 2′,3′-Dialdehyde of ATP - a specific, irreversible inhibitor of component A3 of the methylreductase system of *Methanobacterium thermoautotrophicum*. *J. Bacteriol. 169*, 1737−1739.
(197) Rouviere, P. E., and Wolfe, R. S. (1989) Component A3 of the methylcoenzyme-M methylreductase system of *Methanobacterium thermoautotrophicum*-Delta-H - Resolution into 2 components. *J. Bacteriol. 171*, 4556−4562.
(198) Kuhner, C. H., Lindenbach, B. D., and Wolfe, R. S. (1993) Component-A2 of methylcoenzyme-M reductase system from *Methanobacterium thermoautotrophicum* Delta-H - Nucleotide-sequence and functional expression by *Escherichia coli*. *J. Bacteriol. 175*, 3195−3203.
(199) Rouviere, P. E., Bobik, T. A., and Wolfe, R. S. (1988) Reductive activation of the methyl coenzyme M methylreductase system of *Methanobacterium thermoautotrophicum* Delta-H. *J. Bacteriol. 170*, 3946−3952.
(200) Zhou, Y. Z., Dorchak, A. E., and Ragsdale, S. W. (2013) In vivo activation of methyl-coenzyme M reductase by carbon monoxide. *Front. Microbiol. 4*, 1−9.
(201) Olson, K. D., Mcmahon, C. W., and Wolfe, R. S. (1991) Photoactivation of the 2-(methylthio)ethanesulfonic acid reductase from *Methanobacterium*. *Proc. Natl. Acad. Sci. U. S. A. 88*, 4099−4103.
(202) Wang, Y., Wegener, G., Hou, J., Wang, F., and Xiao, X. (2019) Expanding anaerobic alkane metabolism in the domain of Archaea. *Nat. Microbiol. 4*, 595−602.
(203) Borrel, G., Adam, P. A., McKay, L. J., Chen, L. X., Sierra-García, I. N., Sieber, C. M. K., Letourneur, Q., Ghozlane, A., Andersen, G. L., Li, W. J., Hallam, J. S., Muyzer, G., de Oliveira, V. M., Inskeep, W. P., Banfield, J. F., and Gribaldo, S. (2019) Wide diversity of methane and short-chain alkane metabolisms in uncultured archaea. *Nat. Microbiol. 4*, 603−613.
(204) McKay, L. J., Dlakic, M., Fields, M. W., Delmont, T. O., Eren, A. M., Jay, Z. J., Klingelsmith, K. B., Rusch, D. B., and Inskeep, W. P. (2019) Co-occurring genomic capacity for anaerobic methane and dissimilatory sulfur metabolisms discovered in the Korarchaeota. *Nat. Microbiol. 4*, 614−622.

DOI: 10.1021/acs.biochem.9b00164
Biochemistry 2019, 58, 5198−5220

NOTE ADDED IN PROOF

At the time of the galley proofs three important metagenomic studies of previously uncharacterized, sediment-inhabiting archaeal lineages were published.[202−204] They revealed that the presence of mcr genes and of other methanogenesis related genes in archaea not belonging to the known methanogenic archaea are more widespread than outlined in the sections "Role of MCR in the carbon cycle" and "MCR phylogeny".

DOI: 10.1021/acs.biochem.9b00164
Biochemistry 2019, 58, 5198−5220